Electric Power Systems Research 180 (2020) 106039

Contents lists available at ScienceDirect

Electric Power Systems Research

journal homepage: www.elsevier.com/locate/epsr

The role of power-to-gas and carbon capture technologies in cross-sector decarbonisation strategies

Mathias Berger[a,*], David Radu[a], Raphaël Fonteneau[a], Thierry Deschuyteneer[b], Ghislain Detienne[b], Damien Ernst[a]

[a] Department of Electrical Engineering and Computer Science, University of Liège, Allée de la Découverte 10, 4000 Liège, Belgium
[b] Fluxys, Brussels, Belgium

ARTICLE INFO

Keywords:
Power-to-gas
Gas storage
Integrated energy systems
Optimal system planning
Hydrogen integration
Carbon capture

ABSTRACT

This paper proposes an optimisation-based framework to tackle long-term centralised planning problems of multi-sector, integrated energy systems including electricity, hydrogen, natural gas, synthetic methane and carbon dioxide. The model selects and sizes the set of power generation, energy conversion and storage as well as carbon capture technologies minimising the cost of supplying energy demand in the form of electricity, hydrogen, natural gas or synthetic methane across the power, heating, transportation and industry sectors whilst accounting for policy drivers, such as energy independence, carbon dioxide emissions reduction targets, or support schemes. The usefulness of the model is illustrated by a case study evaluating the potential of sector coupling via power-to-gas and carbon capture technologies to achieve deep decarbonisation targets in the Belgian context. Results, on the one hand, indicate that power-to-gas can only play a minor supporting role in cross-sector decarbonisation strategies in Belgium, as electrolysis plants are deployed in moderate quantities whilst methanation plants do not appear in any studied scenario. On the other hand, given the limited renewable potential, post-combustion and direct air carbon capture technologies clearly play an enabling role in any decarbonisation strategy, but may also exacerbate the dependence on fossil fuels.

1. Introduction

The effective integration of energy systems relying on different vectors is envisioned to hold great promise for better integrating renewable energy sources into energy systems and achieving deep decarbonisation objectives [1].

On the one hand, the very large-scale deployment of technologies harnessing renewable energy sources for electricity generation has often lead to large amounts of curtailed electricity [2] and an accrued need for short and long-term storage capacities in the power system to balance volatile as well as seasonal renewable production patterns. As no electrical, electrochemical, thermal or mechanical storage options (besides perhaps hydroelectric reservoirs, including pumped-storage hydroelectricity) currently offer cheap, grid-scale, long-term storage, and given the fact that in some regions, very large-scale gas storage facilities are available for low-cost, long-term storage, power-to-gas technologies have been proposed as a complement to standard power generation and storage technologies [3,4]. On the other hand, in order to significantly reduce carbon dioxide emissions, sectors such as heating, transportation and industry should also be supplied with low-carbon energy. In this respect, synthetic fuels produced through an integrated power-to-gas chain including electrolysis and methanation processes are also envisioned to play a role [5,6].

Against this backdrop, this paper proposes a framework to tackle long-term centralised planning problems of integrated energy systems coupling four carriers and a commodity, namely electricity, hydrogen, natural gas, methane and carbon dioxide. The capacities of power generation, energy conversion as well as short and long-term storage technologies are sized to minimise the cost of supplying energy demands in the form of electricity, hydrogen, and natural gas across the power, heating, transportation and industry sectors. Policy drivers such as energy security and independence, carbon dioxide emission quotas and support schemes for selected technologies are also accounted for. Moreover, a wide range of technological options is considered, including solar photovoltaic panels, on/offshore wind turbines, open and combined-cycle gas turbines, combined heat and power, waste, biomass and nuclear power plants, electrolysis, methanation, steam methane reforming, direct air and post-combustion carbon capture units, as well as battery, pumped-hydro, carbon dioxide, hydrogen and natural gas storage.

* Corresponding author.
E-mail address: mathias.berger@uliege.be (M. Berger).

https://doi.org/10.1016/j.epsr.2019.106039
Received 1 May 2019; Received in revised form 3 August 2019; Accepted 18 September 2019
Available online 09 January 2020
0378-7796/

Nomenclature

Abbreviations

B	battery storage
BM	biomass power plant
CAPEX	capital expenditure
CCGT	combined-cycle gas turbine
CH_4	methane
CHP	combined heat and power plant
CNG	compressed natural gas
CO_2	carbon dioxide
CO_2eq	CO_2-equivalent
DAC	direct air (carbon) capture
E	electricity
EL	electrolysis plant
ENS	energy not served
EV	electric vehicle
FOM	fixed operation and maintenance
GW(h)	gigawatt(hour)
H_2	hydrogen
H_2O	water
kt	kilotonne
kt/h	kilotonne/hour
LNG	liquified natural gas
LP	linear program
M€	million €
MT	methanation plant
NG	natural gas
NK	nuclear power plant
OCGT	open-cycle gas turbine
O_2	oxygen
PCCC	post-combustion carbon capture
PH	pumped-hydro storage
RES	renewable energy sources
PV	photovoltaic (panels)
SMR	steam methane reformer
TSO	transmission system operator
VOM	variable operation and maintenance
VRE	variable renewable energy
W_{on}	onshore wind (turbines)
W_{off}	offshore wind (turbines)
WS	waste power plant

Sets and indices

C_{E}	set of technologies consuming electricity
C_{NG}	set of technologies consuming natural gas
$C_{\mathrm{H_2}}$	set of technologies consuming hydrogen
$C_{\mathrm{CO_2}}$	set of technologies consuming carbon dioxide
d	index of days in optimisation horizon
e	energy carrier index
$\mathcal{E}$	set of energy carriers with balance equation, i.e., $\mathcal{E}$ = {E, NG, H_2}
p	power generation or energy conversion technology (or plant) index
$\mathcal{P}$	set of power generation and energy conversion technologies
$\mathcal{P}_D$	set of dispatchable power generation technologies running on exogenous fuels
$\mathcal{P}_E$	set of technologies producing carbon-free electricity
$\mathcal{P}_E^N$	set of technologies producing electricity and emitting carbon dioxide
$\mathcal{P}_{\mathrm{CO_2}}$	set of technologies emitting carbon dioxide that may be equipped with a post-combustion capture unit
$\mathcal{P}_{\mathrm{H_2}}$	set of technologies producing hydrogen
$\mathcal{P}_R$	set of renewable-based power generation technologies
s	storage technology (or plant) index
$\mathcal{S}$	set of energy storage technologies
$\mathcal{S}^E$	set of electricity storage technologies
$\mathcal{S}^{\mathrm{NG}}$	set of natural gas storage technologies
$\mathcal{S}^{\mathrm{H_2}}$	set of hydrogen storage technologies
$\mathcal{S}^{\mathrm{CO_2}}$	set of carbon dioxide storage technologies
t	time index
$\mathcal{T}$	set of time periods
$\mathcal{T}_D$	set of first time periods of every day in optimisation horizon

Parameters

β^p	maximum capture rate of post-combustion carbon capture process for technology $p \in \mathcal{P}_{\mathrm{CO_2}}$ [–]
χ^s	duration ratio of storage technology $s \in \mathcal{S}$ [–]
Δ_-^p	decremental ramp rate of technology $p \in \mathcal{P}_D$ [GW/h]
Δ_+^p	incremental ramp rate of technology $p \in \mathcal{P}_D$ [GW/h]
δt	discretisation time step [h]
η^p	conversion efficiency of technology $p \in \mathcal{P}\backslash$ {PCCC, DAC}
η^s	self-discharge rate of storage technology $s \in \mathcal{S}$ [–]
$\eta^{s,C}$	charge efficiency of storage technology $s \in \mathcal{S}$ [–]
$\eta^{s,D}$	discharge efficiency of storage technology $s \in \mathcal{S}$ [–]
κ_0^p	pre-installed (power) capacity of technology $p \in \mathcal{P}_R \cup \mathcal{P}_D \cup \mathcal{S}$ [GWh/h]
$\kappa_{e,t}^{\mathrm{IE}}$	maximum exchange capacity for any carrier $e \in \mathcal{E} \cup \{\mathrm{CO_2}\}$ [GWh/h] or [kt/h]
$\kappa_{\max}^p$	maximum capacity of technology $p \in \mathcal{P}_R$ that may be installed [GWh/h]
$\lambda_{e,t}$	exogenous demand for carrier $e \in \mathcal{E}$ at $t \in \mathcal{T}$ [GWh/h]
$\lambda_{E,d}^{\mathrm{TR}}$	daily electricity demand from electric vehicles [GWh]
μ^p	minimum output power level of technology $p \in \mathcal{P}$ [–]
ν^p	specific CO_2 emissions of fuel on which technology $p \in \mathcal{P}_{\mathrm{CO_2}}$ runs [kt/GWh]
ν_{NG}	specific CO_2 emissions of natural gas [kt/GWh]
π_t^p	normalised production profile value for technology $p \in \mathcal{P}_R$ at time $t \in \mathcal{T}$ [–]
$\phi^{p,CC}$	electrical energy required per unit mass of CO_2 captured via PCCC for technology $p \in \mathcal{P}_{\mathrm{CO_2}}$ [GWh/kt]
ϕ_E^{DAC}	electrical energy required per unit mass of CO_2 captured via DAC [GWh/kt]
$\phi_{\mathrm{NG}}^{\mathrm{DAC}}$	natural gas energy required per unit mass of CO_2 captured via DAC [GWh/kt]
ϕ^{SMR}	electrical energy required per unit energy of H_2 produced via SMR [–]
Π_c	molar mass of carrier/commodity $c \in$ {CH_4, CO_2, H_2, H_2O, O_2, CO_2} [g/mol]
$\Phi_{\mathrm{CO_2}}$	CO_2 emissions quota [kt]
Ψ_e	import budget for carrier $e \in \mathcal{E}$ [GWh]
$\rho_{\mathrm{CO_2/CH_4}}$	ratio of stoichiometric coefficients of CO_2 and CH_4 in the methanation reaction [–]
$\rho_{\mathrm{H_2O/H_2}}$	ratio of stoichiometric coefficients of H_2O and H_2 in the water electrolysis reaction [–]
$\rho_{\mathrm{O_2/H_2}}$	ratio of stoichiometric coefficients of O_2 and H_2 in the water electrolysis reaction [–]
σ^s	minimum state of charge of storage technology $s \in \mathcal{S}$ [–]
Σ_0^s	pre-installed energy capacity of storage technology $s \in \mathcal{S}$ [GWh]
$\Sigma_{\max}^s$	maximum energy capacity of storage technology $s \in \mathcal{S}$ [GWh]
τ	number of time periods in a day
$\theta_{\mathrm{CO_2}}$	specific cost of CO_2 emissions [M€/kt]
$\theta_{e,t}^{\mathrm{IE}}$	economic value of carrier/commodity $e \in \mathcal{E} \cup \{\mathrm{CO_2}\}$ at time $t \in \mathcal{T}$ [M€/GWh]

θ_e^{ENS} value of lost load for carrier $e \in \mathcal{E}$ [M€/GWh]
θ_f^p FOM cost for technology $p \in \mathcal{P}$ [M€/GWh/h]
$\theta_f^{s,K}$ power-related FOM for technology $s \in \mathcal{S}$ [M€/GWh/h]
$\theta_f^{s,S}$ energy-related FOM for technology $s \in \mathcal{S}$ [M€/GWh]
θ_{fuel}^p fuel cost of technology $p \in \mathcal{P}_D$ [M€/GWh]
θ_{SS}^p incentive given for producing one unit of energy with technology $p \in \mathcal{P}$ (support scheme) [M€/GWh]
θ_v^p VOM cost of technology $p \in \mathcal{P}$ [M€/GWh]
$\varkappa_{\mathrm{CH_4}}$ higher heating value of CH_4 [GWh/kt]
$\varkappa_{\mathrm{H_2}}$ higher heating value of H_2 [GWh/kt]
ζ^p CAPEX of technology $p \in \mathcal{P}$ [M€/GWh/h]
$\zeta^{s,K}$ power capacity CAPEX of storage technology $s \in \mathcal{S}$ [M€/GWh/h]
$\zeta^{s,S}$ energy capacity CAPEX of storage technology $s \in \mathcal{S}$ [M€/GWh]

Variables

C_e^{IE} net economic value resulting from trade of carrier/commodity $e \in \mathcal{E} \cup \{CO_2\}$ [M€]
C_e^{ENS} total cost of energy not served for carrier $e \in \mathcal{E}$[M€]
C_{fuel}^p total fuel cost for technology$p \in \mathcal{P}_D$ [M€]
C^p total cost for technology$p \in \mathcal{P}$, incl. CAPEX, FOM, VOM and excl. fuel cost and carbon tax [M€]
C_{SS}^p revenue from support scheme for technology $p \in \mathcal{P}$ [M€]
$E_{e,t}^s$ state of charge of storage technology $s \in \mathcal{S}$, in the form of carrier $e \in \mathcal{E} \cup \{CO_2\}$, at time $t \in \mathcal{T}$ [kt]
$K_{\mathrm{CO_2}}^{p,\mathrm{CC}}$ capacity of post-combustion carbon capture unit equipping technology $p \in \mathcal{P}_{\mathrm{CO_2}}$ [kt/h]
K_E^p capacity of power generation technology $p \in \mathcal{P}_E \cup \mathcal{P}_E^N$ [GWh/h]
K_E^{EL} capacity of electrolysis plants (electrical side) [GWh/h]
K^s power capacity of storage technology $s \in \mathcal{S}$ [GWh/h]
$K_{CO_2}^{DAC}$ capacity of direct air capture units [kt/h]
$K_{H_2}^{SMR}$ capacity of steam methane reforming plants (hydrogen output) [GWh/h]
$K_{CH_4}^{MT}$ capacity of methanation plants (methane output) [GWh/h]
$L_{e,t}^{\mathrm{ENS}}$ energy not served for carrier $e \in \mathcal{E}$ at time $t \in \mathcal{T}$ [GWh/h]
$L_{E,t}^{\mathrm{TR}}$ electricity demand for EVs at time $t \in \mathcal{T}$ [GWh/h]
$P_{\mathrm{CH_4},t}^{\mathrm{MT}}$ CH_4 output of methanation units at time $t \in \mathcal{T}$ [GWh/h]
$P_{E,t}^p$ electricity production/consumption of technology $p \in \mathcal{P}_E \cup \mathcal{P}_E^N \cup C_{\mathrm{E}} \cup \{\mathrm{SMR}\} \cup \mathcal{S}_E$ at time $t \in \mathcal{T}$ [GWh/h]
$P_{E,t}^{p,N}$ net electricity production/consumption of technology $p \in \mathcal{P}_E^N \cup \{\mathrm{SMR}\}$ at time $t \in \mathcal{T}$ [GWh/h]
$P_{e,t}^{\mathrm{IE}}$ net exchange flow of carrier $e \in \mathcal{E}$ at time t [GWh/h]
$P_{e,t}^I$ imports of carrier $e \in \mathcal{E}$ at time t [GWh/h]
$P_{e,t}^E$ exports of carrier $e \in \mathcal{E}$ at time t [GWh/h]
$P_{\mathrm{H_2},t}^p$ hydrogen production/consumption of technology $p \in \mathcal{P}_{\mathrm{H_2}} \cup C_{\mathrm{H_2}} \cup \mathcal{S}_{\mathrm{H_2}}$ at time $t \in \mathcal{T}$ [GWh/h]
$P_{\mathrm{NG},t}^p$ natural gas consumption of technology $p \in C_{\mathrm{NG}}$ at time $t \in \mathcal{T}$ [GWh/h]
$P_{e,t}^{s,C}$ charge flow of carrier $e \in \mathcal{E}$ in storage technology $s \in \mathcal{S}$, at time $t \in \mathcal{T}$ [GWh/h]
$P_{e,t}^{s,D}$ discharge flow of carrier $e \in \mathcal{E}$ in storage technology $s \in \mathcal{S}$, at time $t \in \mathcal{T}$ [GWh/h]
$P_{e,t}^s$ net flow of carrier $e \in \mathcal{E}$ in storage technology $s \in \mathcal{S}$ at time $t \in \mathcal{T}$ [GWh/h]
$Q_{\mathrm{CO_2},t}^p$ CO_2 mass flow produced by technology $p \in \mathcal{P}_{\mathrm{CO_2}}$ at time $t \in \mathcal{T}$ [kt/h]
$Q_{\mathrm{CO_2},t}^{c,A}$ fraction of CO_2 mass flow of technology $p \in \mathcal{P}_{\mathrm{CO_2}}$ released into atmosphere at time $t \in \mathcal{T}$ [kt/h]
$Q_{\mathrm{CO_2},t}^{c,\mathrm{CC}}$ fraction of CO_2 mass flow of technology $p \in \mathcal{P}_{\mathrm{CO_2}}$ captured via PCCC at time $t \in \mathcal{T}$ [kt/h]
$Q_{\mathrm{CO_2},t}^{\mathrm{DAC}}$ CO_2 mass flow exiting DAC units at time $t \in \mathcal{T}$ [kt/h]
$Q_{\mathrm{CO_2},t}^{\mathrm{DAC},A}$ CO_2 mass flow captured from atmosphere via DAC at time $t \in \mathcal{T}$ [kt/h]
$Q_{\mathrm{CO_2},t}^I$ CO_2 mass flow imports at time $t \in \mathcal{T}$ [kt/h]
$Q_{\mathrm{CO_2},t}^E$ CO_2 mass flow exports at time $t \in \mathcal{T}$ [kt/h]
$Q_{\mathrm{CO_2},t}^{\mathrm{IE}}$ net CO_2 mass flow exchange at time $t \in \mathcal{T}$ [kt/h]
$Q_{\mathrm{CO_2},t}^{\mathrm{MT}}$ mass inflow of CO_2 required by methanation plants at time $t \in \mathcal{T}$ [kt/h]
$Q_{\mathrm{CO_2},t}^s$ net CO_2 mass flow from storage technology $s \in \mathcal{S}_{\mathrm{CO_2}}$ at time $t \in \mathcal{T}$ [kt/h]
$Q_{\mathrm{H_2O},t}^{\mathrm{EL}}$ mass inflow of H_2O into electrolysis plants at time $t \in \mathcal{T}$ [kt/h]
$Q_{\mathrm{O_2},t}^{\mathrm{EL}}$ mass outflow of O_2 from electrolysis plants at time $t \in \mathcal{T}$ [kt/h]
S^s energy capacity of storage technology s [GWh]

The problem is formulated as a linear program (LP) assuming perfect foresight over the optimisation horizon and perfect competition, with high degrees of temporal and techno-economic detail to accurately represent power system operation under high renewable penetration [7]. Investment decisions are made at the initial time instant and no discounting of future money flows is performed. Moreover, an optimisation horizon of five years with investment costs reduced to five-year equivalents is used to approximate the problem over the full planning horizon of 20 years, thus reducing the computational burden. The planning and operational problems are solved concurrently, thereby yielding optimal sizes and operational schedules for all technologies. Finally, the framework is applied to the Belgian energy system in order to explore future configurations leading to substantial carbon dioxide emission reductions across sectors.

The remainder of this paper is organised as follows. Section 2 reviews related works on the operation and planning of integrated energy systems, and highlights the areas to which the present paper contributes. Section 3 describes the proposed optimisation formulation, and a case study exploring future configurations of the Belgian energy system is presented in Section 4. Finally, Section 5 concludes the paper and future work avenues are discussed.

2. Related works

The topic of integrated energy systems has recently received considerable attention in the academic literature [10]. Early contributions include Bakken and Holen [11], Geidl and Andersson [12] and Mancarella and Chicco [13], which focus on planning, operational and economic aspects of integrated energy systems, respectively. These themes have since developed into key areas of integrated energy systems research. In this section, relevant studies considering the operation of integrated energy systems are briefly reviewed before planning problems and models of interest are discussed.

The operational challenges and opportunities arising from the coupling of the electricity and natural gas systems have been the focus of several papers [3,14–25]. More precisely, the coupling of electricity and gas systems via gas-fired power plants has been investigated in [14–20,24,25], which consider the impact of scheduling strategies and carrier physics on the reliability and performance of coupled systems. Furthermore, the effect of system coupling via power-to-gas technologies on system operation has been analysed by Belderbos [3], Clegg and Mancarella [21], Qadrdan et al. [22] and Li et al. [23]. The operational implications of shifting some of the heat demand from gas to electricity for both networks have also been studied by Qadrdan et al. [26].

Although studying the operation of integrated energy systems

provides a better understanding of opportunities and challenges stemming from the integration of different carriers, it falls short of indicating how key system components, especially energy transmission, conversion and storage technologies, should be designed to realise the full potential of system integration. Hence, such analyses must be complemented with (long-term) planning studies, which are reviewed next.

Building upon the energy hub concept introduced by Geidl et al. [12], the same authors propose a framework to tackle integrated energy hub operation and layout problems including storage elements [27]. Though suitable for power generation, energy conversion and storage technology selection, the method does not identify optimal sizes for the selected technologies and relies on a nonlinear, nonconvex optimisation problem, thus proving impractical for long planning horizons. In [28], the authors investigate the deployment of batteries, power-to-gas (producing synthetic methane directly) and seasonal storage to complement standard dispatchable and renewable-based power generation technologies, but model details are not given. An updated model, based on a LP formulation and including hydrogen and carbon dioxide carriers, is presented in [3] but only considers the power sector and a yearly planning horizon. An explicit treatment of the long-term storage problem is made by Gabrielli et al. [29], where a methodology is introduced to reduce the computational burden of planning problems including such technologies, handled via a mixed-integer linear programming formulation. A yearly optimisation horizon is considered, which limits design robustness with respect to yearly weather variations. In [16,30–35], variations on the joint expansion planning problem of electricity and gas systems are tackled, for instance including random outages and uncertain electricity load forecasts [30], endogenous nodal gas price formation mechanisms [16], uncertain active and reactive power demands in electricity distribution systems [32], the possibility to build electricity storage [34] or power-to-gas as well as reliability criteria [35]. Such problems are computationally challenging, and the temporal resolution used is generally low. The computational complexity is further reduced by the use of convex relaxations [16], a low spatial resolution [31] and decomposition methods [30,32–35]. Despite providing highly valuable insight into how the operation of integrated energy systems influences their design, and partly owing to computational limitations, these studies do not consider the sizing of renewable-based power generation technologies, focus on two carriers and sectors only, and generally fail to assess the environmental merits of the resulting system designs, e.g., in terms of carbon dioxide emissions reductions. Finally, Pleßmann et al. [4], Brown et al. [6], Brown and Hörsch [36], Dominkovic et al. [37] have investigated the energy and technology mix which would be needed to achieve deep decarbonisation goals in different regions. In particular, in [4] the amount of energy storage in the form of battery, high-temperature thermal and gas (methane) storage that would be required to power the global electricity demand with 100% renewable energy is assessed. A LP formulation is invoked but not presented, which makes results interpretation difficult. In [6] and [36], Brown et al. provide a comprehensive power system planning model including hydrogen and synthetic methane energy carriers and also considering the transportation and heating sectors. The model is spatially and temporally resolved and also includes policy constraints in the form of a carbon dioxide emissions budget. However, an optimisation horizon of a single year and a restricted set of technologies are considered, whilst the industry sector is not accounted for. In [37], the energy system design which would lead to a zero carbon system in Southeast Europe is studied via the ENERGYPLAN model. The latter is not spatially resolved, while the optimisation horizon spans a single year.

In summary, building upon our previous work [8], this paper adds to the literature on the planning of integrated energy systems (i) by providing a detailed, highly interpretable and computationally efficient long-term, multi-sector, integrated energy system model along with an open-source Python implementation and comprehensive data resources [9], (ii) by reporting on a case study focussing on a realistic energy system and quantifying the extent to which power-to-gas technologies and sector coupling may help achieve deep decarbonisation goals.

3. Problem statement and formulation

In this section, the planning problem is stated, the scope of the model is described along with a set of modelling assumptions, and a mathematical formulation is proposed.

3.1. Problem statement

This paper focuses on the long-term planning of multi-sector, integrated energy systems featuring power generation, energy conversion and storage assets, with a view to identify cost-optimal energy system configurations capable of supplying energy demand across sectors in the form of different energy vectors whilst satisfying a set of pre-specified technical and regulatory constraints, e.g. adequacy, reliability or environmental performance targets.

In its full complexity, this problem involves (i) all major existing and promising energy vectors, (ii) all sectors of the economy, (iii) a detailed spatial representation of the underlying energy systems, (iv) a multi-scale time horizon combining long-term, discrete investment decisions with short-term operational ones, (v) an accurate description of the physics and control systems of the underlying carrier networks, (vi) an accurate representation of generation, conversion and storage technologies down to the level of individual plants, (vii) short- and long-run uncertainty.

From a practical perspective, considering all aforementioned features simultaneously results in an intractable model. Hence, choices must be made depending on the scope and intended use of the model, as discussed next.

3.2. Model scope

In this paper, the emphasis is put on formulating a high-level multi-sector, integrated energy system model with high interpretability and very good tractability. More precisely, a model is sought that allows to quickly evaluate how technology options, policy choices, cost or technical performance assumptions impact energy system design and energy carrier flow patterns. As this paper focusses particularly on the role and integration of RES, power-to-gas, carbon capture and storage (also seasonal storage) technologies, key model attributes include a multi-year planning horizon with high temporal resolution, a high level of techno-economic detail and a wide range of technology options, carriers and sectors. Key simplifying assumptions are reviewed next.

3.3. Modelling assumptions

Centralised Planning. Investment decisions are made by a central planner, who also operates the energy system, and whose goal is to minimise the cost of supplying energy demand across sectors in the form of various energy vectors.

Investment & operational decisions. A single, multi-year investment horizon is considered. Investment decisions are made at the beginning of the time horizon and assets are immediately available. Operational decisions are made at hourly or sub-hourly time steps of the investment horizon. The investment and operational problems are solved simultaneously.

Spatial aggregation. The energy system is represented by a single node, and the physics of energy carrier networks is reduced to a single nodal balance equation.

Perfect foresight & knowledge. The central planner has perfect foresight and knowledge, that is, future weather and load patterns, as well as all technical and economic parameters are known with certainty. In other words, no uncertainty of any nature is considered.

Linearity of technology models. All technologies and individual plants are represented via linear input-output mathematical models, i.e., conversion and storage processes are described in energy terms, and the inherently nonlinear and nonconvex relationships representing these processes are replaced by linear approximations. Input or output dynamics are considered for some technologies, but only storage technologies have a simple state space representation. Given the multi-year time horizon, high temporal resolution, high number of technological options and carriers considered, directly introducing nonlinear or nonconvex technology models would greatly complicate and slow the solution procedure, or make the problem intractable altogether.

3.4. Model formulation

3.4.1. Technologies

In the sequel, for the sake of clarity, technology models are presented in a generic fashion. Depending on the application, they may be used to describe individual plants or technology classes, and instantiated accordingly. It is worth emphasising that no assumption pertaining to the aggregation of individual plants into technology classes is made nor required to formulate the model.

Noncontrollable renewable technologies. A set $\mathcal{P}_R = \{\text{PV}, W_{\text{on}}, W_{\text{off}}\}$ of noncontrollable, renewable-based power generation technologies is considered, including solar PV, onshore and offshore wind turbines. The constraints describing the operation and sizing of these technologies can be expressed as

$$P^p_{E,t} \leq \pi^p_t(\kappa^p_0 + K^p_E), \quad \forall\, t \in \mathcal{T}, \quad \forall\, p \in \mathcal{P}_R, \tag{1}$$

$$K^p_E \leq \kappa^p_{\max}, \quad \forall\, p \in \mathcal{P}_R, \tag{2}$$

while investment and operating costs write as

$$C^p = (\zeta^p + \theta^p_f)K^p_E + \sum_{t\in\mathcal{T}} \theta^p_v P^p_{E,t}\delta t, \quad \forall\, p \in \mathcal{P}_R. \tag{3}$$

Eq. (1) describes the power generation from RES plants and their sizing, where an inequality has been used to allow for curtailment. Eq. (2) expresses the fact that the renewable potential is finite within the boundaries of the system considered. Eq. (3) gives the basic cost structure for investing in and operating technologies harnessing RES, including capital expenditure (CAPEX), fixed operation and maintenance (FOM) and variable operation and maintenance (VOM) costs. FOM costs represent the capacity-based share of operating costs, whereas VOM costs represent the fraction of operating costs dependent upon the amount of power produced. This structure is applicable to most technologies discussed in this paper, and exclude fuel costs and CO_2 emission levies. Finally, it is worth mentioning that curtailment is not penalised, as curtailed production has already been indirectly paid for through investment and operating expenses, and it would otherwise provide an artificial incentive to build technologies reducing it.

Dispatchable technologies with exogenous fuels. A set $\mathcal{P}_D = \{\text{BM}, \text{WS}, \text{NK}\}$ of dispatchable power generation technologies relying on exogenous fuels to produce electricity is considered, comprising biomass, waste, and nuclear power plants. Constraints describing the operation and sizing of these technologies, $\forall\, t \in \mathcal{T}$, write as

$$P^p_{E,t} \leq \kappa^p_0 + K^p_E, \quad \forall\, p \in \mathcal{P}_D, \tag{4}$$

$$P^p_{E,t} - P^p_{E,t-1} \leq \Delta^p_+(\kappa^p_0 + K^p_E), \quad \forall\, p \in \mathcal{P}_D, \tag{5}$$

$$P^p_{E,t} - P^p_{E,t-1} \geq -\Delta^p_-(\kappa^p_0 + K^p_E), \quad \forall\, p \in \mathcal{P}_D, \tag{6}$$

$$\mu^p(\kappa^p_0 + K^p_E) \leq P^p_{E,t}, \quad \forall\, p \in \mathcal{P}_D, \tag{7}$$

$$Q^p_{\text{CO}_2,t} = \frac{\nu^p P^p_{E,t}}{\eta^p}, \quad p \in \{\text{BM}, \text{WS}\}, \tag{8}$$

whereas costs can be expressed as

$$C^p_{\text{fuel}} = \sum_{t\in\mathcal{T}} \frac{\theta^p_{\text{fuel}} P^p_{E,t}\delta t}{\eta^p}, \quad \forall\, p \in \mathcal{P}_D, \tag{9}$$

$$C^p_{\text{CO}_2} = \sum_{t\in\mathcal{T}} \theta_{\text{CO}_2} Q^p_{\text{CO}_2,t}\delta t, \quad \forall\, p \in \{\text{BM}, \text{WS}\}. \tag{10}$$

Eq. (4) describes the sizing of dispatchable power generation technologies running on exogenous fuels. The sizing variable is the output electrical power. Eqs. (5) and (6) describe ramping constraints (up and down, respectively) on the electrical power output. Eq. (7) enforces must-run constraints for selected technologies. Eq. (8) gives the carbon dioxide mass flow generated by the operation of biomass and waste power plants. Eqs. (9) and (10) provide an expression for fuel costs and costs incurred by technologies emitting carbon dioxide, e.g., as a result of the implementation of a carbon tax or an emissions trading scheme. The remainder of the costs can be expressed via Eq. (3).

Exchanges of carriers and commodities. Both imports and exports of carriers and commodities are envisaged. Let $\mathcal{E} = \{\text{E}, \text{NG}, \text{H}_2\}$. Then, the equations describing the exchange of carriers and commodities,$\forall\, t \in \mathcal{T}$, write as

$$P^{\text{IE}}_{e,t} = P^I_{e,t} - P^E_{e,t}, \quad \forall\, e \in \mathcal{E}, \tag{11}$$

$$Q^{\text{IE}}_{\text{CO}_2,t} = Q^I_{\text{CO}_2,t} - Q^E_{\text{CO}_2,t}, \tag{12}$$

$$-\kappa^{\text{IE}}_{e,t} \leq P^{\text{IE}}_{e,t} \leq \kappa^{\text{IE}}_{e,t}, \quad \forall\, e \in \mathcal{E} \tag{13}$$

$$-\kappa^{\text{IE}}_{\text{CO}_2,t} \leq Q^{\text{IE}}_{\text{CO}_2,t} \leq \kappa^{\text{IE}}_{\text{CO}_2,t}, \tag{14}$$

$$C^{\text{IE}}_e = \sum_{t\in\mathcal{T}} \theta^{\text{IE}}_{e,t} P^{\text{IE}}_{e,t}\delta t, \quad \forall\, e \in \mathcal{E} \tag{15}$$

$$C^{\text{IE}}_{\text{CO}_2} = \sum_{t\in\mathcal{T}} \theta^{\text{IE}}_{\text{CO}_2,t} Q^{\text{IE}}_{\text{CO}_2,t}\delta t. \tag{16}$$

Eq. (11) decomposes the net exchange of carriers into import and export variables. This decomposition is warranted as import or export variables appear on their own in policy constraints. Eq. (12) defines the same decomposition for carbon dioxide imports and exports. Eqs. (13) and (14) express that the levels of imports and exports of carriers and commodities are constrained, and the maximum exchange capacity may vary in time. Eqs. (15) and (16) describe the money flows resulting from the exchange of carriers and commodities, which may represent revenues or costs.

Electrolysis plants. Electrolysis plants produce hydrogen and oxygen from water using an electrical current. The constraints describing their operation and sizing, $\forall\, t \in \mathcal{T}$, write as

$$P^{\text{EL}}_{\text{H}_2,t} = \eta^{\text{EL}} P^{\text{EL}}_{E,t}, \tag{17}$$

$$P^{\text{EL}}_{E,t} \leq K^{\text{EL}}_E, \tag{18}$$

$$\mu^{\text{EL}}\eta^{\text{EL}} K^{\text{EL}}_E \leq P^{\text{EL}}_{\text{H}_2,t}, \tag{19}$$

$$Q^{\text{EL}}_{\text{H}_2\text{O},t} = \rho_{\text{H}_2\text{O}/\text{H}_2} \frac{\Pi_{\text{H}_2\text{O}}}{\Pi_{\text{H}_2}} \frac{P^{\text{EL}}_{\text{H}_2,t}}{\varkappa_{\text{H}_2}}, \tag{20}$$

$$Q^{\text{EL}}_{\text{O}_2,t} = \rho_{\text{O}_2/\text{H}_2} \frac{\Pi_{\text{O}_2}}{\Pi_{\text{H}_2}} \frac{P^{\text{EL}}_{\text{H}_2,t}}{\varkappa_{\text{H}_2}}. \tag{21}$$

Eq. (17) describes the conversion process in terms of the electrical power input and the chemical energy contained in gaseous hydrogen, whereas Eq. (18) sizes the electrolysis plants. The sizing variable is the maximum electrical input power. Eq. (19) constrains the minimum hydrogen output level [38]. Eqs. (20) and (21) give the water consumption and oxygen production resulting from the production of hydrogen by water electrolysis. Though usually disregarded in power-to-gas studies, it is particularly insightful to track these quantities, as they will inherently feature in any power-to-gas strategy and possibly impact its feasibility or cost. Some of these quantities may also be subject to,

e.g., policy constraints. The costs associated with electrolysis plants have the standard structure given in Eq. (3).

Fuel cells. Fuel cells produce water and electricity from hydrogen and oxygen. The constraints describing their operation and sizing, $\forall\, t \in \mathcal{T}$, write as

$$P^{\mathrm{FC}}_{E,t} = \eta^{\mathrm{FC}} P^{\mathrm{FC}}_{\mathrm{H}_2,t}, \tag{22}$$

$$P^{\mathrm{FC}}_{E,t} \leq K^{\mathrm{FC}}_{E}, \tag{23}$$

$$\mu^{\mathrm{FC}} K^{\mathrm{FC}}_{E} \leq P^{\mathrm{FC}}_{E,t}. \tag{24}$$

Eq. (22) describes the conversion process, in terms of the chemical energy in the hydrogen input stream and the electrical output power. Eq. (23) sizes the fuel cell power plants, with the maximum output electrical power taken as the sizing variable. Eq. (24) constrains the minimum output power of the fuel cell power plants [38]. The oxygen consumption and water production are evaluated in a fashion similar to Eqs. (20) and (21). Finally, the cost structure of fuel cell power plants is that described in Eq. (3).

Gas turbines. Gas turbines rely on natural gas to produce electricity, releasing carbon dioxide in the process. The constraints describing their operation and sizing, $\forall\, t \in \mathcal{T}$, write as

$$P^{p}_{E,t} = \eta^{p} P^{p}_{\mathrm{NG},t}, \quad \forall\, p \in \{\mathrm{OCGT},\, \mathrm{CCGT}\}, \tag{25}$$

$$P^{p}_{E,t} \leq K^{p}_{E}, \quad \forall\, p \in \{\mathrm{OCGT},\, \mathrm{CCGT}\}, \tag{26}$$

$$Q^{p}_{\mathrm{CO}_2,t} = \nu^{p} P^{p}_{\mathrm{NG},t}, \quad \forall\, p \in \{\mathrm{OCGT},\, \mathrm{CCGT}\}, \tag{27}$$

and ramping constraints can also be included by adding inequalities (5) and (6). Eq. (25) represents the conversion process, linking the electrical power output to the chemical energy of the natural gas burnt. Eq. (26) describes the sizing of the gas-fired power plants, where the sizing variable is the maximum electrical power output. Eq. (27) gives the carbon dioxide emissions resulting from the operation of gas turbines. Finally, the cost of investing in and operating natural gas-fired power plants can be obtained via Eqs. (3) and (10). Fuel expenditure does not factor directly in these costs as natural gas is an endogenous carrier, and these expenses are indirectly reflected by natural gas import costs.

Methanation plants. Methanation plants consume hydrogen and carbon dioxide to produce synthetic methane. The constraints describing their operation and sizing, $\forall\, t \in \mathcal{T}$, write as

$$P^{\mathrm{MT}}_{\mathrm{CH}_4,t} = \eta^{\mathrm{MT}} P^{\mathrm{MT}}_{\mathrm{H}_2,t}, \tag{28}$$

$$P^{\mathrm{MT}}_{\mathrm{CH}_4,t} \leq K^{\mathrm{MT}}_{\mathrm{CH}_4}, \tag{29}$$

$$\mu^{\mathrm{MT}} K^{\mathrm{MT}}_{\mathrm{CH}_4} \leq P^{\mathrm{MT}}_{\mathrm{CH}_4,t}, \tag{30}$$

$$Q^{\mathrm{MT}}_{\mathrm{CO}_2,t} = \rho_{\mathrm{CO}_2/\mathrm{CH}_4} \frac{\Pi_{\mathrm{CO}_2}}{\Pi_{\mathrm{CH}_4}} \frac{P^{\mathrm{MT}}_{\mathrm{CH}_4,t}}{\varkappa_{\mathrm{CH}_4}}. \tag{31}$$

Eq. (28) describes the conversion process, in terms of the chemical energy of the input and output carriers, whilst Eq. (29) represents the sizing of the methanation plants. The sizing variable is the maximum synthetic methane (energy) output. Eq. (30) expresses the fact that some methanation technologies must be run continuously [38]. Eq. (31) gives the consumption of carbon dioxide required to produce synthetic methane. Finally, the cost structure for methanation plants is that already presented in Eq. (3).

Steam methane reformers. Steam methane reformers consume natural gas and electricity (to drive compressors feeding high-pressure natural gas to the reforming reactor [39–41]) to produce hydrogen, and also emit carbon dioxide. The constraints describing their operation and sizing, $\forall\, t \in \mathcal{T}$, can be expressed as

$$P^{\mathrm{SMR}}_{\mathrm{H}_2,t} = \eta^{\mathrm{SMR}} P^{\mathrm{SMR}}_{\mathrm{NG},t}, \tag{32}$$

$$P^{\mathrm{SMR}}_{E,t} = \phi^{\mathrm{SMR}} P^{\mathrm{SMR}}_{\mathrm{H}_2,t}, \tag{33}$$

$$Q^{\mathrm{SMR}}_{\mathrm{CO}_2,t} = \nu_{NG} P^{\mathrm{SMR}}_{\mathrm{NG},t}, \tag{34}$$

$$P^{\mathrm{SMR}}_{\mathrm{H}_2,t} \leq K^{\mathrm{SMR}}_{\mathrm{H2}}. \tag{35}$$

Eq. (32) describes the conversion process from natural gas to hydrogen, expressed in terms of the chemical energy of input and output gases, whereas Eq. (33) gives the electrical power consumption required to produce hydrogen. Eq. (34) represents the carbon dioxide emissions from the process, as the vast majority of the natural gas used both as fuel and feedstock is converted into carbon dioxide and vented [41]. Eq. (35) sizes the SMR plants, where the sizing variable is the maximum hydrogen energy output. The cost structure of steam methane reformers can be expressed as in Eqs. (3) and (10).

Direct air carbon capture. This process requires the consumption of electricity and natural gas to remove carbon dioxide from the atmosphere [42]. The constraints describing the operation and sizing of direct air capture (DAC) units, $\forall\, t \in \mathcal{T}$, write as

$$P^{\mathrm{DAC}}_{E,t} = \phi^{\mathrm{DAC}}_{E} Q^{\mathrm{DAC},A}_{\mathrm{CO}_2,t}, \tag{36}$$

$$P^{\mathrm{DAC}}_{\mathrm{NG},t} = \phi^{\mathrm{DAC}}_{\mathrm{NG}} Q^{\mathrm{DAC},A}_{\mathrm{CO}_2,t}, \tag{37}$$

$$Q^{\mathrm{DAC}}_{\mathrm{CO}_2,t} = Q^{\mathrm{DAC},A}_{\mathrm{CO}_2,t} + \nu_{NG} P^{\mathrm{DAC}}_{\mathrm{NG},t}, \tag{38}$$

$$Q^{\mathrm{DAC},A}_{\mathrm{CO}_2,t} \leq K^{\mathrm{DAC}}_{\mathrm{CO}_2}. \tag{39}$$

Eqs. (36) and (37) describe the electrical power and natural gas consumption required by the technology to capture carbon dioxide from the atmosphere. Eq. (38) defines the total carbon dioxide mass flow exiting the DAC system, including the carbon dioxide captured directly from the atmosphere and that resulting from the combustion of natural gas fuel. Eq. (39) describes the sizing of DAC units, where the sizing variable is the maximum mass flow of carbon dioxide that may be removed from the atmosphere. Finally, the costing of this technology is performed using the standard structure in Eq. (3).

Post-combustion carbon capture. Post-combustion carbon capture (PCCC) units can be fitted onto technologies whose operation relies on the combustion of fossil fuels and therefore emits carbon dioxide [43]. In essence, post-combustion capture units run on electricity and capture a fraction, typically up to 90%, of the carbon dioxide emitted by the technology they complement. Let $\mathcal{P}_{\mathrm{CO}_2} = \{\mathrm{BM},\, \mathrm{WS},\, \mathrm{OCGT},\, \mathrm{CCGT},\, \mathrm{CHP},\, \mathrm{SMR}\}$ be the set of technologies which may be fitted with a PCCC unit. Then, the constraints representing the operation and sizing of capture units associated with any $d \in \mathcal{P}_{\mathrm{CO}_2}$, $\forall\, t \in \mathcal{T}$, can be expressed as

$$Q^{p}_{\mathrm{CO}_2,t} = Q^{p,\mathrm{CC}}_{\mathrm{CO}_2,t} + Q^{p,A}_{\mathrm{CO}_2,t}, \tag{40}$$

$$Q^{p,\mathrm{CC}}_{\mathrm{CO}_2,t} \leq \beta^{p} Q^{p}_{\mathrm{CO}_2,t}, \tag{41}$$

$$P^{p,\mathrm{CC}}_{E,t} = \phi^{p} Q^{p,\mathrm{CC}}_{\mathrm{CO}_2,t}, \tag{42}$$

$$Q^{p,\mathrm{CC}}_{\mathrm{CO}_2,t} \leq K^{p,\mathrm{CC}}_{\mathrm{CO}_2}, \tag{43}$$

Eq. (40) is the carbon dioxide mass flow balance, with a fraction of the CO_2 emitted being captured whilst the remainder is released into the atmosphere. Eq. (41) constrains the captured mass flow, as given by the maximum capture rate. Eq. (42) represents the electricity consumption of the capture units. Eq. (43) describes the sizing of the system, where the sizing variable is the maximum carbon dioxide mass flow which may be captured. The cost structure is the standard one already introduced in Eq. (3).

The use of post-combustion carbon capture technologies reduces the power output of power generation technologies and further increases the power consumption of technologies not producing any electricity, e.g. SMR. Hence, the net power generation or consumption of these technologies, $\forall\, t \in \mathcal{T}$, can be expressed as

$$P^{p,N}_{E,t} = P^{p}_{E,t} - P^{p,\mathrm{CC}}_{E,t}, \quad p \in \mathcal{P}_{\mathrm{CO}_2} \backslash \{\mathrm{SMR}\}, \tag{44}$$

$$P^{\mathrm{SMR},N}_{E,t} = P^{\mathrm{SMR,CC}}_{E,t} + P^{\mathrm{SMR}}_{E,t}. \tag{45}$$

Storage technologies. A set of storage technologies for various carriers and commodities is considered. The constraints describing the operation and sizing of those technologies, $\forall\, t \in \mathcal{T}$, write as

$$\sigma^s(\Sigma^s_0 + S^s) \le E^s_{e,t} \le (\Sigma^s_0 + S^s) \le \Sigma^s_{\max}, \quad s \in \mathcal{S}, \tag{46}$$

$$E^s_{e,t} = \eta^s E^s_{e,t-1} + \eta^{s,C} P^{s,C}_{e,t} \delta t - P^{s,D}_{e,t} \delta t / \eta^{s,D}, \quad s \in \mathcal{S}, \tag{47}$$

$$P^{s,D}_{e,t} \le \kappa^s_0 + K^s, \quad \forall\, s \in \mathcal{S}, \tag{48}$$

$$P^{s,C}_{t} \le \gamma^s(\kappa^s_0 + K^s), \quad \forall\, S \in \mathcal{S}, \tag{49}$$

$$P^{s}_{e,t} = -P^{s,C}_{e,t} + P^{s,D}_{e,t}, \quad \forall\, s \in \mathcal{S}. \tag{50}$$

Eq. (46) describes the sizing of the energy storage capacity, while constraining the minimum storage level. Eq. (47) represents the charge and discharge dynamics of storage systems. Eqs. (48) and (49) enforce bounds on charge and discharge rates, which may be asymmetric, and size the power capacity of the storage system. Eq. (50) gathers charge and discharge variables into a single net exchange variable. Sometimes, the energy and power capacities of storage systems may not be sized independently from one another, in which case a constraint of the form

$$K^s = S^s / \chi^s, \tag{51}$$

may be enforced. Finally, the costs of investing in and operating storage technologies can be expressed as

$$C^s = (\zeta^{s,S} + \theta^{s,S}_f) S^s + (\zeta^{s,K} + \theta^{s,K}_f) K^s, \quad \forall\, s \in \mathcal{S} \backslash \{\mathcal{S}_{\mathrm{CO_2}}\}, \tag{52}$$

where a distinction is made between energy and power capacities, which is particularly relevant in the case of batteries [44]. A similar cost structure is applied to carbon dioxide storage technologies. In this paper, it is assumed that operating costs only have a capacity-based component. If need be, revising this assumption is straightforward.

3.4.2. Carrier physics

For notational simplicity, let $\mathcal{P}_E = \{\mathrm{PV}, W_{\mathrm{on}}, W_{\mathrm{off}}, \mathrm{NK}, \mathrm{FC}\}$, $\mathcal{P}^N_E = \mathcal{P}_{\mathrm{CO_2}} \backslash \{\mathrm{SMR}\}$ and $C_{\mathrm{E}} = \{\mathrm{EL}, \mathrm{DAC}\}$. Then, the physics of the electricity carrier is reduced to a system-wide power balance equation,

$$\sum_{p \in \mathcal{P}_E} P^p_{E,t} + \sum_{p \in \mathcal{P}^N_E} P^{p,N}_{E,t} + \sum_{s \in \mathcal{S}_E} P^s_{E,t} + P^{\mathrm{IE}}_{E,t} + L^{\mathrm{ENS}}_{E,t} = \lambda_{E,t} + L^{\mathrm{TR}}_{E,t} + \sum_{p \in C_{\mathrm{E}}} P^p_{E,t} + P^{\mathrm{SMR},N}_{E,t}, \quad \forall\, t \in \mathcal{T}. \tag{53}$$

It is worth mentioning that in this model, the electricity demand $L^{\mathrm{TR}}_{E,t}$ from electric vehicles (EV) is not completely exogenous. Indeed, it is assumed that the timing and intensity of EV charging can be optimised over the course of the day, subject to the constraint that a daily supply level is guaranteed,

$$\sum_{t=0}^{\tau-1} L^{\mathrm{TR}}_{E,h+t} \delta t = \lambda^{\mathrm{TR}}_{E,h}, \quad \forall\, h \in \mathcal{T}_D. \tag{54}$$

This modelling approach is backed up by field test results, which have shown that electric vehicles spend more than 90% of their time parked [45], and the development of smart charging strategies [46,47], provided that the underlying infrastructure is available. At any rate, the impact of these assumptions will be discussed in the results section. Now, for the natural gas system, the system-wide balance writes as

$$P^{\mathrm{MT}}_{\mathrm{CH_4},t} + \sum_{s \in \mathcal{S}_{\mathrm{NG}}} P^s_{\mathrm{NG},t} + P^{\mathrm{IE}}_{\mathrm{NG},t} + L^{\mathrm{ENS}}_{\mathrm{NG},t} = \lambda_{\mathrm{NG},t} + \sum_{p \in C_{\mathrm{NG}}} P^p_{\mathrm{NG},t}, \quad \forall\, t \in \mathcal{T}. \tag{55}$$

A balance equation is also considered for the hydrogen carrier, such that

$$\sum_{p \in \mathcal{P}_{\mathrm{H_2}}} P^p_{\mathrm{H_2},t} + \sum_{s \in \mathcal{S}_{\mathrm{H_2}}} P^s_{\mathrm{H_2},t} + P^{\mathrm{IE}}_{\mathrm{H_2},t} + L^{\mathrm{ENS}}_{\mathrm{H_2},t} = \lambda_{\mathrm{H_2},t} + \sum_{p \in C_{\mathrm{H_2}}} P^p_{\mathrm{H_2},t}, \quad \forall\, t \in \mathcal{T}. \tag{56}$$

For the carbon dioxide commodity, the following balance equation is employed

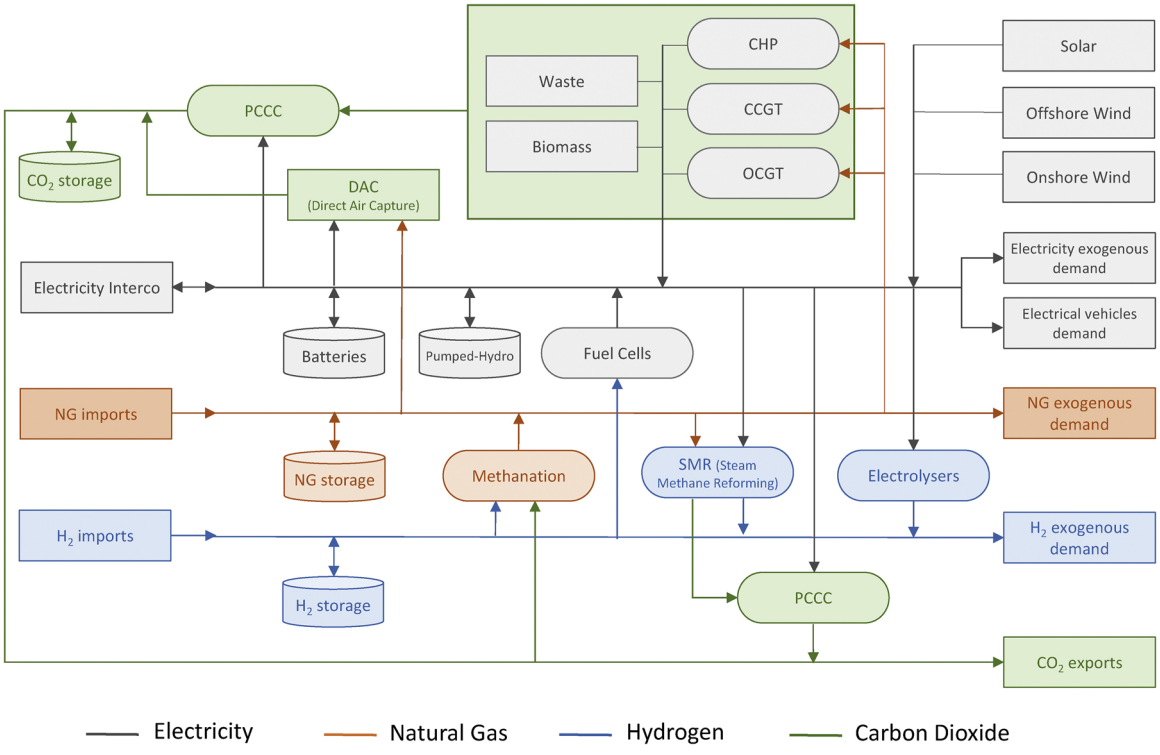

Fig. 1. Schematic of the energy system model, where arrows show the direction of carrier and commodity flows as defined by technology characteristics.

$$\sum_{p\in\mathcal{P}_{\mathrm{CO_2}}} Q^{p,\mathrm{CC}}_{\mathrm{CO_2},t} + Q^{\mathrm{DAC}}_{\mathrm{CO_2},t} + \sum_{s\in S_{\mathrm{CO_2}}} Q^{s}_{\mathrm{CO_2},t} + Q^{\mathrm{IE}}_{\mathrm{CO_2},t} = \sum_{p\in C_{\mathrm{CO_2}}} Q^{p}_{\mathrm{CO_2},t}, \quad \forall\, t\in\mathcal{T}. \tag{57}$$

It is worth noticing that no exogenous carbon dioxide demand is considered. Moreover, emissions released into the atmosphere do not appear in Eq. (57). Instead, they appear in a carbon quota constraint introduced in the next subsection. Finally, briefly discussing the slack variables $L^{\mathrm{ENS}}_{e,t}$ introduced in energy balance equations for $e\in\mathcal{E}$ is in order. These variables maintain the feasibility of the optimisation problem even if the exogenous energy demands cannot be satisfied in full, e.g., if a severe carbon constraint is enforced, no carbon capture technologies are available and the renewable potential is insufficient. Since shedding load is only permitted as a last resort, these variables are (heavily) penalised in the objective

$$C^{\mathrm{ENS}}_{e} = \sum_{t\in\mathcal{T}} \theta^{\mathrm{ENS}}_{e} L^{\mathrm{ENS}}_{e,t}\delta t, \quad \forall\, e\in\mathcal{E}, \tag{58}$$

and the penalty values reflect, to some extent, how desirable system adequacy is.

3.4.3. Policy drivers

Three types of policy drivers are modelled, namely energy import and CO_2 emissions quotas, as well as support schemes. Energy import quotas can be simply expressed via an inequality constraint

$$\sum_{t\in\mathcal{T}} P^{I}_{e,t}\delta t \le \Psi_{e}, \quad \forall\, e\in\mathcal{E}. \tag{59}$$

Similarly, the CO_2 emissions quota constraint can be written as

$$\sum_{t\in\mathcal{T}} [\nu_{\mathrm{NG}}(\lambda_{\mathrm{NG},t} - L^{\mathrm{ENS}}_{\mathrm{NG},t}) - Q^{\mathrm{DAC},A}_{\mathrm{CO_2},t} + \sum_{p\in\mathcal{P}_{\mathrm{CO_2}}} Q^{p,A}_{\mathrm{CO_2},t}]\delta t \le \Phi_{\mathrm{CO_2}}. \tag{60}$$

Support schemes promoting the deployment of selected technologies are assumed to reward their use, thus offsetting some of their operating costs rather than reducing their capital expenditure from the outset. More formally, for any eligible technology $p\in\mathcal{P}$ producing carrier e, the existence of a support scheme can be modelled via

$$C^{p}_{\mathrm{SS}} = -\sum_{t\in\mathcal{T}} \theta^{p}_{\mathrm{SS}} P^{p}_{e,t}\delta t, \tag{61}$$

where θ^{p}_{SS} represents the value of the incentive given for the production of one unit of carrier e by technology d and must be nonnegative. This way of modelling support schemes is akin to green certificates systems or feed-in premiums used in some European countries.

3.4.4. Planning model

The objective function, to be minimised, is formed by summing costs in Eqs. (3), (9), (10), (15), (16), (52), (58) and (61) for all relevant technologies, carriers and commodities. All other equations are used as constraints to describe the operation and sizing of the system, carrier physics and policy drivers. As a reminder, an optimisation horizon of five years with investment costs reduced to five-year equivalents is used to approximate the full planning horizon of 20 years and reduce the computational burden. The resulting model, represented schematically in Fig. 1, is implemented in Pyomo (Python) and readily available as open-source software [9]. The model is solved with IBM ILOG CPLEX 12.8 in around 1800 s (on average) on a custom workstation with two Intel Xeon Gold 6140 2.3 GHz processors and 256 GB of RAM operating under CentOS. Since the parallel computing capabilities of the workstation were not used, the model could also be run on a laptop, though the exact solving time is expected to be longer and will eventually depend upon laptop computing power.

4. Case study

This section shows the applicability and usefulness of the model with a case study considering future configurations of a realistic energy system. The case study is briefly introduced, before the data used to instantiate to model is described. Results are then presented and discussed.

4.1. Description

The case study explores future configurations of the Belgian energy system and assesses the potential of renewable-based power generation, carbon capture and sector coupling technologies such as power-to-gas to achieve deep, cross-sector decarbonisation objectives. The sectors targeted for emissions reductions include power generation, road and electrified rail transport (thus excluding aviation and shipping), heating (residential, commercial and industrial), as well as industrial subsectors consuming hydrogen and natural gas, as the latter may be replaced by synthetic methane. Five scenarios are studied, and each scenario aims at identifying the system configuration minimising the cost of supplying demands for electricity, hydrogen and natural gas across all aforementioned sectors as the scope of technological options is progressively broadened. These scenarios therefore provide insight into the interactions between different technologies and their respective impact on energy system design. More precisely, the first scenario investigates the case in which the Belgian nuclear fleet is entirely decommissioned and no carbon capture technology of any kind is available. The second scenario evaluates the benefits of maintaining half of the nuclear fleet in the absence of carbon capture technologies. The next three scenarios disregard nuclear, and focus instead on the influence of carbon capture technologies. More accurately, the third scenario assumes the availability of post-combustion carbon capture units whereas the fourth scenario considers both post-combustion and direct air capture technologies. Finally, the renewable potential constraints are relaxed in the fifth scenario, in order to assess the economic competitiveness of RES in the presence of carbon capture technologies. The carbon dioxide emissions target is uniform across scenarios and the only technologies whose capacity is kept constant throughout all scenarios are combined heat and power, biomass, waste and pumped-hydro power plants. This is supported by the fact that these technologies are already deployed in the Belgian power system, and no plans to increase the capacity of these technologies any further clearly feature in current Belgian energy policy [48]. At any rate, the aforementioned dispatchable technologies have higher specific emissions than natural gas, and as a result of the carbon budget constraint, these technologies would be unlikely to play a prominent role even if they were sized.

4.2. Data

In this subsection, the data used to build the case study is described, starting with renewable generation profiles and energy consumption, before the carbon budget, energy/commodity imports and exports as well as key economic and technical parameters are introduced.

4.2.1. Renewable generation profiles

Generation profiles for variable renewable energy (VRE) resources, i.e. solar PV, onshore and offshore wind, are retrieved from transmission system operator (TSO) databases [49]. The measurements, which originally have a quarter–hourly resolution and span five consecutive years (2014–2018), are re-sampled to a hourly resolution by a standard averaging procedure. As a result, signal variations occurring on sub-hourly time scales are smoothed out. The re-sampled profile is then normalised by the installed capacity available at the corresponding hour, which is also provided by the TSO.

4.2.2. Energy consumption

Time series of electricity demand in Belgium are obtained from estimations made by the Belgian TSO [50] and include electrical loads at both transmission and distribution levels, excluding future (exogenous) heating and transportation demands considered in the model, which are discussed later. An averaging method is used to re-sample raw data with quarter-hourly resolution, covering five full calendar years (2014–2018), into hourly-sampled time series normalised by the peak load of each year, which are then concatenated. These time series are then scaled to have an estimated peak value of 13.5 GW, which corresponds to a situation with little change in future electricity use [48]. Then, the yearly electricity demand of the system varies between 86.2 and 89.2 TWh, depending on the year considered.

Natural gas demand for residential and commercial purposes is retrieved from the electronic data platform of the Belgian natural gas TSO [51] at hourly resolution and covering the same time horizon as the electricity demand time series. Processed data represents the aggregated load associated with the low- (L-gas) and high-calorific (H-gas) natural gas networks in Belgium. Yearly demand ranges between 79.5 and 92.8 TWh, depending on the calendar year.

Moreover, the model includes an exogenous electricity demand profile corresponding to the heating of residential and commercial spaces, and replacing a total of 38 TWh of petroleum products currently in use [52] and emitting substantial amounts of CO_2. Switching to cleaner fuels, e.g. natural gas, is usually cumbersome as these consumers are most often located in rural or semi-rural areas without any access to the gas distribution network. However, given their efficiency and affordability, heat pumps may be an option to decarbonise this sector. Hence, a heat pump technology with a flat coefficient of performance (COP) of 2 is assumed to supply this segment of the heating demand, the profile of which is assumed to be the same as that of the heating demand supplied by natural gas.

In this paper, the extent to which the industry sector can be decarbonised is limited to those subsectors employing natural gas, e.g. for hydrogen production via steam methane reforming, industrial heating or as a feedstock. Hourly-sampled historical (i.e. 2014–2018) demand time series available on the electronic data platform of the Belgian gas system operator are used [51]. Similarly to the residential and commercial sectors, the input time series represent the aggregated load associated with both low- and high-calorific natural gas networks. The energy demand from industry is less dependent on annual temperature variations and, depending on the year studied, the total yearly consumption varies between 41.1 and 46.0 TWh. In fact, as given in [51], the profile includes the demand from existing steam methane reforming plants, which is not reported as such. Hence, the estimated natural gas demand from steam methane reforming is computed from the documented yearly hydrogen production capabilities via SMR on the Belgian territory, which amount to 5.7 TWh/year [53]. These plants usually supply industries running continuous processes. Thus, a flat hourly profile of 0.65 GWh/h is formed and deducted from the original profile [51] in order to obtain the industrial natural gas demand time series used to instantiate the model.

In addition, the existing yearly hydrogen demand in Belgium is estimated to be around 18 TWh [54], which is supplied by a mix of local production via the aforementioned SMR plants and imports from France and the Netherlands [55]. The Belgian industries relying on hydrogen, mostly the petrochemical and fertiliser industries, are known to rely largely on continuous chemical processes and thus operate in near-continuous, steady regimes. Hence, a constant 2 GWh/h hydrogen demand is considered, and the hydrogen demand profile used in the model is flat.

As far as the transportation sector is concerned, the model includes the (electrified) rail and road transport energy demand shares. The former is already included in data retrieved from the electricity TSO [50]. Regarding the latter, in 2015, there were close to 7.2 million vehicles registered in Belgium (incl. personal vehicles, utility vehicles, lorries, motorcycles and buses) [55], with an estimated 95.6 TWh demand of petroleum products only [52], emitting over 25.7 Mt CO2eq on a yearly basis [56]. In this paper, it is assumed that the entire fleet of diesel- and gasoline-fuelled vehicles is replaced by a fleet of equal size with equal numbers of cars running on compressed natural gas (CNG), hydrogen (fuel cell vehicles) and electric power (EV). Hourly demand profiles for CNG- and fuel cell-based vehicles are derived from confidential data measured by the natural gas operator at CNG refuelling stations and up-scaled to the fleet size. For electric vehicles, a synthetic daily demand profile is built assuming an average energy efficiency of the underlying technology of 0.2 kWh/km and flat daily week-day and week-end travel distances of 50 and 20 km, respectively.

Typical daily aggregated profiles of electricity, natural gas and hydrogen demand are displayed in Fig. 2.

4.2.3. CO_2 budget

The present model includes the power generation, residential and commercial, as well as road and electrified rail transport sectors in their

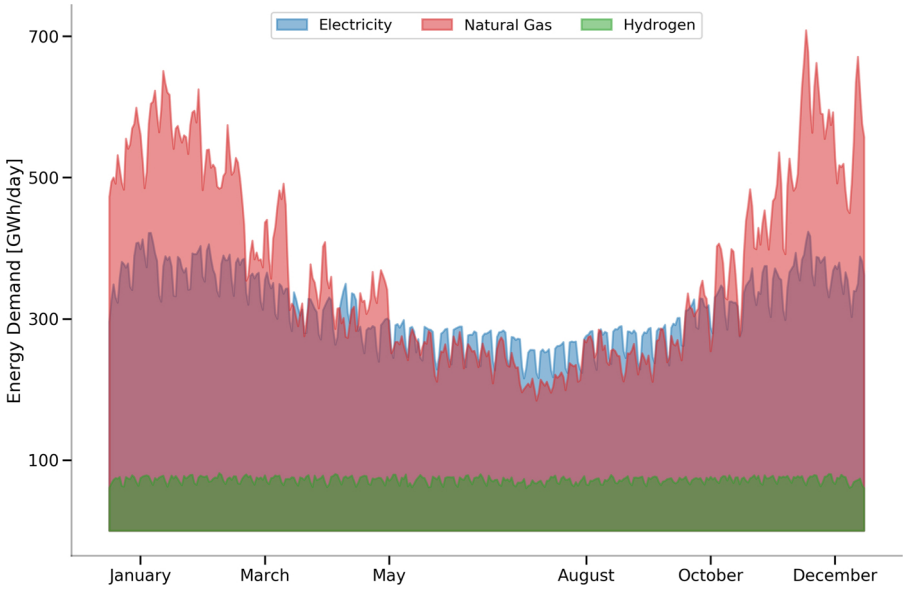

Fig. 2. Daily aggregated profiles of electricity, natural gas and hydrogen demand in a typical year.

entirety, while only the industrial subsectors consuming natural gas and hydrogen are taken into account. According to [56], in 1990, the first three sectors were responsible for the emission of 23.6, 20.0 and 25.0 Mt CO_2eq, respectively, while emissions associated with the natural gas-based share of industry is estimated to be around 9.0 Mt CO_2eq, also accounting for some hydrogen production. The latter figure is obtained based on a 45 TWh demand of natural gas in the industrial sector [52] and an associated 0.2 tCO_2eq/MWh_{th} specific emission value [57]. Thus, the 1990 CO_2 reference emissions level for the system studied with the proposed model amounts to 77.6 Mt CO_2eq, or 51.8% of total national emissions at the time. The carbon dioxide budget considered in all scenarios is set to achieve a reduction of 80% from 1990 levels, or 15.5 Mt/yr.

4.2.4. Imports & exports of energy & commodity

In this case study, both electricity imports and exports are considered, whereas only imports of natural gas and hydrogen and exports of carbon dioxide, respectively, are envisaged.

The electricity import/export capacity is set to 6.5 GW, which is consistent with planned interconnection developments in the 2020s [48]. In addition, the annual electricity imports allowed in the model correspond to roughly 11.5 TWh, amounting to approximately 10% of the total, cross-sector annual electrical load. The costs of electricity imports/exports are based on wholesale prices from the ELIX index of EPEX [9]. This assumption is further discussed later on.

The natural gas import capacity is set to 90 GW, which roughly corresponds to the input capacity of the Belgian natural gas network. The annual imports budget is virtually unconstrained. The natural gas import price time series is derived from medium-term forecasts for the Belgian gas hub, computed and provided by the Belgian natural gas TSO. The Belgian gas hub is particularly well-connected and can resort to a variety of supply options, resulting in an average natural gas price around 12€/MWh in the case at hand.

The import of hydrogen is assumed to be in the form of multi-weekly hydrogen deliveries by tankers. Tankers are assumed to have a capacity of 10^5 m^3 and transport hydrogen compressed at 700 bars, such that each tanker delivers 165 GWh over the course of 24 hours. It is further assumed that at most three fixed delivery slots are available each week, which is consistent with the 110 slots made available at the liquefied natural gas (LNG) terminal at Zeebrugge in 2018. As a result, maximum annual hydrogen imports total 25.74 TWh. The hydrogen import cost is estimated to be around 160€/MWh [9]. It is worth mentioning that no hydrogen terminal currently exists in Belgium but estimating the associated costs is beyond the scope of this study, as the primary goal is to assess the extent to which hydrogen imports are favoured over local production.

Finally, it is assumed that carbon dioxide can be exported to a sequestration site at a maximum rate of 3.5 kt/h, such that roughly 30 Mt can be exported annually. Volumetric flows corresponding to this export rate are equal to 9×10^3 m^3/h for supercritical carbon dioxide or 1.13×10^5 m^3/h for gaseous carbon dioxide at 15 MPa and 283.15 K [58], which is the pressure at which carbon dioxide exits the direct air capture process [42]. The cost of exporting and sequestrating 1 t of carbon dioxide is estimated to be around 2€ [43]. The export rate assumption will be found to have a non-negligible impact on results and will therefore be further discussed later.

4.2.5. Key economic and technical parameters

The main technical and economic parameters of the technologies available in the proposed model are shown in Table 1. A complete list of all parameter values along with references is provided in [9]. At this stage, making a few comments about values displayed in Table 1 is in order.

For power generation technologies, the electrical efficiency is provided. For conversion technologies, the overall process efficiency is listed. For storage technologies, the round-trip efficiency is given, while batteries also have a non-negligible self-discharge rate, shown in parentheses. For carbon capture technologies, the value represents the maximum share of CO_{-2} that may be captured.

All CAPEX are expressed per unit of power capacity (GW) for all dispatchable and conversion technologies, energy capacity (GWh) for storage technologies except carbon dioxide, or flow rate (kT/h) for carbon capture and storage technologies, respectively. Fixed O&M costs are reported on a yearly basis using the same units. Variable O&M costs exclude fuel expenses and are reported per unit energy (GWh). The carbon dioxide storage system is assumed to be a man-made, industrial-sized CO_2 buffer of 100 kt. Its CAPEX is expressed per kt of CO_2 stored.

The cost of post-combustion carbon capture technologies depends on the fuel that is used by the underlying technology. In this regard, a distinction is made between technologies running on natural gas, e.g. OCGT, CCGT, CHP, SMR, and others, e.g. biomass and waste power plants, for which a coal-based post-combustion carbon capture set-up

Table 1
Key technical and economic parameters of technologies considered. Units are discussed in Section 4.2.5.

	κ_0 (κ_{max}) GW/GWh/kT h^{-1}	η %	CAPEX M€	FOM (VOM) M€	Lifetime years
Solar PV	4.0 (40.0)		510	22.3 (N/A)	30
Onshore wind	2.8 (8.4)		910	37.8 (N/A)	30
Offshore wind	2.3 (8.0)		2,000	8.8 (N/A)	30
Gas-fired plants (CCGT)	0.0 (13.5)	58.0	830	27.8 (0.0042)	25
Gas-fired plants (OCGT)	0.0 (13.5)	41.0	560	18.6 (0.0042)	25
CHP	1.8 (N/A)	49.0		40.0 (0.0)	
Waste PP	0.3 (N/A)	22.7		175.6 (0.0248)	
Biomass PP	0.9 (N/A)	28.1		102.9 (0.0051)	
Hydrogen fuel cell	0.0 (13.5)	50.0	2,000	100.0 (0.0)	10
Electrolyser	0.0 (13.5)	62.0	600	30.0 (0.0)	15
Methanation plants	0.0 (13.5)	78.0	400	20.0 (0.0)	20
Steam methane reformers	0.0 (13.5)	80.0	400	20.0 (0.0)	20
Post-combustion CC (NG)	0.0 (4,000.0)	90.0	3,150		20
Post-combustion CC (other)	0.0 (2,000.0)	90.0	2,160		20
Direct air CC	0.0 (1,000.0)		7,500	25.0 (0.0)	30
Battery storage (p)	0.0 (2,500.0)		108	5.4 (0.0)	20
Battery storage (e)	0.0 (5,000.0)	85.0 (99.9)	326	16.3 (0.0)	10
Pumped-hydro storage (p)	1.3 (N/A)				
Pumped-hydro storage (e)	5.3 (N/A)	81.0		45.0 (0.008)	
Hydrogen storage (e)	0.0 (10,000.0)	96.4	11	0.55 (0.0)	30
Natural gas storage (e)	8,000.0 (N/A)	99.0		0.0025 (0.0)	
Carbon dioxide storage	0.0 (100.0)		0.1		20

was used as a proxy in the estimation of associated costs.

Though not shown in Table 1, the costs of energy not served (also known as value of lost load) for electricity, hydrogen and natural gas are set to 3000€/MWh, 500€/MWh and 500€/MWh, respectively. The value used for electricity is consistent with values reported for private end users [59] (Fig. 3, left panel in the aforementioned reference), although lower than those listed for economic (industrial) consumers. From a modelling standpoint, however, the values must also be selected to promote adequacy, i.e. the costs incurred when failing to serve the energy demand should exceed the investment and operating costs required to deploy, operate and maintain technologies allowing to supply the energy demands. In particular, the value of lost load is set higher for electricity than for other carriers as the electricity system must be balanced at all times, whereas local imbalances can be tolerated in the gas system. Bearing this in mind, the values for natural gas and hydrogen were selected after consulting the Belgian natural gas TSO. Finally, a carbon price of 80€/t has been applied in each scenario.

4.3. Results

Fig. 3 displays the installed capacities of all technologies which are sized in each scenario. Hence, CHP, biomass, waste and pumped-hydro power plants, whose capacities are fixed and shown in Table 1, do not appear in Figure 3. Then, Tables 2–4 gather the capacities of carbon capture and storage technologies, system and energy costs, broken down by carrier, as well as volumes of energy imports and energy demand not served, respectively. In Table 3, the system-wide cost includes all investment and operating costs, as well as all expenses stemming from energy and commodity imports/exports, and energy demand not served. The costs of carriers are reported solely with respect to the corresponding volumes of demand served. Thus, for any given carrier, its cost is obtained by dividing the expenses resulting from all technologies producing it and importing it by the demand for this carrier that was served. Moreover, when deployed, PCCC costs are included in electricity and hydrogen costs. Carbon dioxide costs are obtained by computing PCCC and DAC costs and dividing by the amount of CO_2 captured. Finally, it is worth mentioning that DAC costs are reported without energy-related expenses. Now, general observations are made before results are analysed and discussed for each scenario.

Firstly, the renewable potential is fully exploited in each of the first four scenarios, which explains the fact that the installed capacity of renewable-based power generation technologies only changes in scenario 5. Furthermore, the total installed capacity of dispatchable power generation, shown in Fig. 3, remains remarkably constant across all

Table 2
Post-combustion and direct air carbon capture deployments for each of the five scenarios. Figures representing capture rates are expressed in kt/h.

	S1	S2	S3	S4	S5
Technology					
OCGT	N/A	N/A	0.0	0.0	0.0
CCGT	N/A	N/A	3.07	2.55	1.84
CHP	N/A	N/A	0.31	0.13	0.13
Biomass	N/A	N/A	0.0	0.0	0.0
Waste	N/A	N/A	0.08	0.08	0.08
SMR	N/A	N/A	0.71	0.03	0.69
Direct Air CC	N/A	N/A	N/A	1.90	1.60

Table 3
System-wide and electricity (E), natural gas (NG), hydrogen (H_2) and carbon dioxide (CO_2) sub-system costs associated with the five considered scenarios. Carbon dioxide costs are reported without energy-related expenses.

	Unit	S1	S2	S3	S4	S5
System	b€/year	67.1	50.8	41.2	14.7	9.6
E	€/MWh	67.1	52.4	40.8	46.0	45.6
NG	€/MWh	11.6	11.7	11.8	12.0	12.0
H_2	€/MWh	164.3	146.8	25.0	163.0	24.9
CO_2	€/t	N/A	N/A	35.1	49.2	46.6

Table 4
Import and energy not served (ENS) volumes of electricity (E), natural gas (NG) and hydrogen (H_2) across the five considered scenarios (TWh).

		S1	S2	S3	S4	S5
E	Imports	57.2	57.2	57.2	57.2	57.2
	ENS	0.0	0.0	0.0	0.0	0.0
	Curtailment	1.7	3.4	18.6	8.3	94.7
NG	Imports	365.8	365.8	855.4	1124.6	1124.5
	ENS	545.6	390.8	347.1	0.0	0.0
H_2	Imports	128.7	120.8	0.5	127.9	0.1
	ENS	2.0	1.9	0.0	0.1	0.0

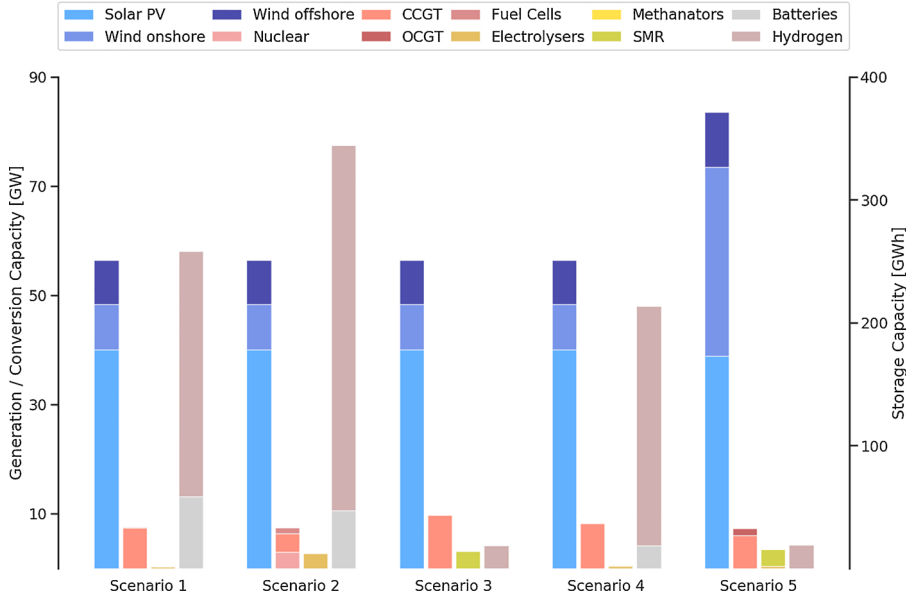

Fig. 3. Deployed generation, conversion and storage capacities across the five considered scenarios. For each scenario, the first, second, third and fourth bars represent renewable-based power generation, dispatchable power generation, other conversion and storage technologies, respectively, besides CO_2 storage.

scenarios, around 10 GW (including CHP, biomass and waste plants), which constitutes approximately 50% of non-EV peak load and implies that even in systems with a ratio of installed renewable capacity to peak load much greater than 1, as in scenario 5, a substantial amount of dispatchable power generation is needed and preferred over storage options like batteries. In addition, the only technology never to feature in any scenario despite being sized is methanation plants. In fact, in order to achieve substantial system-wide CO_2 emissions reductions, emissions are optimised across sectors and carriers. In particular, when carbon capture technologies are not available, most of the hydrogen demand can be supplied with carbon-free imports and electrolysis. Then, the electricity demand can be partly supplied by renewable-based generation but significant (fossil-based) dispatchable capacity is still needed. In other words, without any carbon capture technology and once the renewable potential is fully exploited, the CO_2 emissions resulting from electricity production cannot be further decreased. The use of post-combustion carbon capture only allows to decrease the amount of CO_2 emissions from the electricity sector, which nonetheless remain nonzero, or provide a cheap, low-carbon alternative to hydrogen imports and electrolysis via steam methane reforming. Moreover, synthetic methane, when burnt, releases the same amount of CO_2 as fossil methane, and a number of applications cannot benefit from the use of carbon capture technologies. Hence, since the carbon budget is very small, gas load must be shed and, in the current setup, no incentive for deploying methanation plants exists. When direct air capture technologies are available, however, system-wide atmospheric emissions can be further reduced, and synthetic methane production can be envisaged. Nevertheless, it cannot compete economically with natural gas imports, which have similar applications and properties and cost only 12€/MWh on average. Hence, for the reasons detailed above, energy not served (ENS) in the form of natural gas appears in scenarios 1–3, as can be seen from Table 4. Finally, it is worth mentioning that the maximum capacity of carbon dioxide storage of 100 kt is built in scenarios 3–5.

In scenario 1, as can be seen from Fig. 3, the only dispatchable power generation technologies installed are hydrogen fuel cells (70 MW) and combined cycle gas turbines (7.4 GW), mostly owing to their low specific emissions, in the context of a tight carbon budget and the unavailability of carbon capture technologies. Indeed, all existing polluting dispatchable technologies are run at their minimum level, that is, biomass and waste power plants have a capacity factor of 0% and 20%, respectively, the latter reflecting a must-run constraint. The hydrogen supply consists of imports and 360 MW of electrolysis plants. No steam methane reformers are built as a result of the tight carbon constraint, which is reflected by high hydrogen prices in Table 3. Moreover, the sizing and operation of hydrogen storage plants is mostly driven by unsteady imports and electrolysis supply patterns. Batteries are also built to minimise curtailment, which stands at 1.7 TWh or 0.4% of total renewable electricity generation.

Descriptive statistics relative to the charge of EVs in scenario 1 are shown in Table 5. Firstly, these figures imply that EVs are charged no more than 25% of the time, as percentiles correspond to integer multiples of 1 hour, and suggest that the modelling assumption made earlier is consistent. From a physical standpoint, the values of the 95th and 99th percentiles appear reasonable in the context of upgrades to the power network infrastructure that would be required to accommodate over 50 GW of RES capacity. Even with such upgrades, though, the peak charge of 19.59 GW appears *a priori* excessive. However, estimating the exact cost and technical feasibility of such upgrades is beyond the scope of this paper.

In scenario 2, half of the Belgium nuclear fleet (3 GW), which has already been amortised, is assumed to remain in operation. Nuclear plants therefore provide cheap, carbon-free, base load production, amounting to roughly 26.2 TWh annually. This is essentially equivalent to offsetting the load curve by 3 GW. As a result, the capacity of CCGT is drastically reduced to 3.1 GW, and the spared gas consumption is shifted to non-power demand for natural gas in order to decrease the amount of natural gas energy not served, as shown in Table 4. In addition, more renewable energy can be harvested for hydrogen production as well as subsequent repowering. Hence, nuclear plants indirectly promote the deployment of electrolysis and fuel cell plants, whose capacities increase to 2.8 GW and 1.0 GW, respectively. The hydrogen storage system is sized accordingly, with a capacity higher than that observed in scenario 1. Overall, the cost of supplying hydrogen also decreases, as shown in Table 3, which is consistent with the fact that hydrogen imports decrease by about 1.7 TWh annually. Batteries are still built, though in smaller proportions, and around 3.4 TWh or 0.8% of renewable electricity production is curtailed. The dynamics of battery, hydrogen and natural gas storages are shown in Fig. 4. Battery dynamics appear mostly driven by daily solar PV production patterns, whereas hydrogen storage dynamics display a periodic behaviour characteristic of multi-weekly hydrogen tanker deliveries, although some lower frequency component is also visible. Finally, the natural gas storage system dynamics display a clear seasonal trend and are driven by the price of natural gas, which is higher in the winter and lower in the summer, such that the storage system is emptied over the winter and filled in the summer. It is worth noting that none of these signals possesses a clear seasonal component which is electricity supply-driven.

In scenario 3, the availability of post-combustion carbon capture technologies appears to favour fossil fuel-based technologies. For power generation, technologies harnessing renewables are still deployed, but fuel cells disappear, as a result of their high cost. CCGT capacity increases to 9.8 GW, and plants are equipped with PCCC, as shown in Table 2. It is no longer desirable to minimise curtailment, which amounts to 18.6 TWh or 4.7% of total renewable electricity production, and neither batteries nor electrolysis plants are built. This is consistent with the observation that the entire hydrogen supply comes from steam methane reformers equipped with PCCC and operating with a 95% capacity factor. As Table 3 indicates, the cost of hydrogen is substantially reduced, which also highlights the economic optimum for producing low-carbon hydrogen. As a result, storing hydrogen imports is no longer necessary and the size of the storage system shrinks drastically. In this scenario, around 19.6 Mt of CO_2 are captured and exported annually. It is worth noting that some natural gas energy demand remains unserved, as some applications like commercial or residential heating cannot benefit from PCCC, and the emissions that would result from supplying this demand would exceed the remaining budget, even after cross-sector optimisation.

In scenario 4, direct air capture technologies allow for the removal of CO_2 from the atmosphere, such that the energy demand across carriers and sectors can be served in its entirety, as shown in Table 4. Somewhat counter-intuitively, hydrogen storage, batteries, electrolysis plants and hydrogen imports, which did not feature in scenario 3, resurface here. Interestingly, this can be explained by observing that the carbon dioxide export capacity of 3.5 kt/h is saturated by the influx of CO_2 from power plants equipped with PCCC and DAC, which, for every 1 t of CO_2 removed from the atmosphere produces roughly 1.3 t of gaseous CO_2 ready for further processing. Indeed, 30.6 Mt of CO_2 are exported annually. The effects of the saturation of the export capacity are far-reaching and manifold. Firstly, regarding the electricity supply, both CCGT and associated PCCC capacities decrease to a level where all captured CO_2 can be exported. Minimising curtailment becomes a priority again, and batteries are therefore built along with 390 MW of electrolysis plants, eventually leading to the curtailment of 8.3 TWh or 2% of total renewable electricity generation, down from 4.7% in the

Table 5
Descriptive statistics of EV charging, expressed in GW, for scenario 1.

Mode	Min	p75	p85	p95	p99	Max
0.00	0.00	0.00	2.07	5.44	8.89	19.69

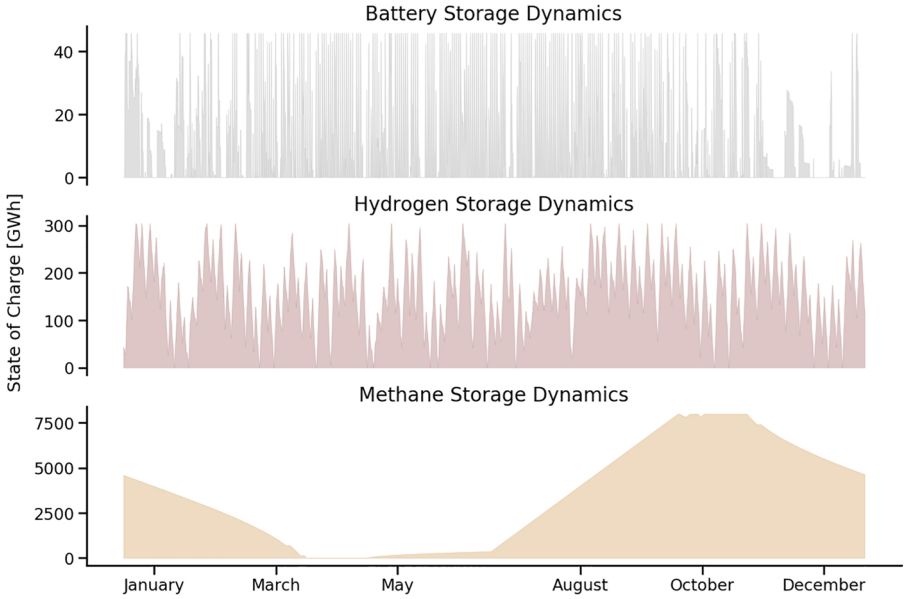

Fig. 4. State of charge dynamics of battery, hydrogen and natural gas storage systems for scenario 2.

previous scenario. Secondly, SMR equipped with PCCC can be barely used, thus only 160 MW are built, and a shift in hydrogen supply therefore occurs from SMR to imports and electrolysis plants, which is reflected in the cost of hydrogen in Table 3. In addition, the hydrogen storage system size is comparable to that found in other scenarios relying on imports and electrolysis. Overall system costs are much lower due to the absence of unserved energy demand.

In scenario 5, the renewable potential constraint is relaxed, and PV capacity decreases slightly to 38.3 GW, whilst both onshore and offshore wind capacities increase to 34.6 GW and 10.0 GW, respectively. This additional RES capacity reduces the role of gas in the power generation mix. Indeed, the fleet of CCGT plants observed in all previous scenarios is replaced by a combination of OCGT and CCGT plants. The former, which have low CAPEX, are only used in peak load situations and rare low-RES production events. These claims are supported by the fact that the capacity factors of OCGT and CCGT plants are around 1.3% and 31.9%, respectively. As discussed previously, the economic performance of the system design largely depends on whether or not SMR can be used, and RES capacity is sized to permit its use, that is, to limit saturation of carbon dioxide exports. Around 470 MW of electrolysis plants appear in this scenario to harvest some additional renewable-based electricity, but the priority is clearly not to avoid curtailment, which stands at 94.7 TWh or 16.1% of renewable electricity production. Overall, this scenario shows that despite strong assumptions on RES costs reduction, these technologies appear unable to supply the electricity demand on their own, as the optimal system design still features fossil fuel-based dispatchable capacity like natural gas-fired power plants.

At this stage, further commenting on Table 3 is in order. It is clear that the system cost steadily decreases from scenario 1 to scenario 5, as the amount of unserved energy demand progressively decreases and the economically-optimal supply mix is achieved for each carrier. For electricity, if nuclear is unavailable, this usually involves a mix of RES and gas-fired power plants equipped with PCCC, but little electrolysis and little to no storage capacity, besides the existing pumped-hydro plants. Then, for hydrogen, steam methane reformers equipped with PCCC appear to constitute the optimum, followed by electrolysis and imports. For natural gas, under the present assumptions, imports constitute the economic optimum and no methanation appears. This line of thought explains the evolution of hydrogen and natural gas costs reported in Table 3. However, the cost of electricity, counter-intuitively, is slightly more expensive in scenario 5 than in scenario 4, and 12% more expensive in scenario 5 than in scenario 3. This observation can in fact be explained by the large amount of curtailed electricity observed in scenario 5, which is equal to 94.7 TWh. Indeed, the RES capacity is oversized to allow for the use of SMR. For curtailment levels comparable to those observed in scenario 3, the cost of electricity would fall around 40€/MWh, which is comparable to that found in scenario 3, and cheaper than that of scenario 4. At any rate, these observations point to nontrivial cross-carrier and cross-sector interactions, which should be carefully considered in energy system design. This especially holds true if all components of the energy system are not upgraded or jointly sized, and particularly if legacy pipeline systems are used for novel applications such as carbon dioxide or hydrogen transport. It is also worth emphasising that even though carbon capture technologies appear to play a key role in meeting ambitious emissions targets, their deployment also exacerbates the dependence on fossil fuels, which may result in a lock-in effect and raises serious questions as to their suitability as a long-term solution.

Finally, it is worth briefly discussing the assumption on annual electricity import quotas. Recall that only 10% of the total annual electricity demand could be imported, which roughly corresponds to a 20% capacity factor for the interconnection. In fact, allowing higher import levels risks jeopardising results informativeness and robustness. Indeed, the interconnection serves as a slack and no modelling of neighbouring countries is performed. In other words, provided that the annual imports budget is not exceeded, 6.5 GW of carbon-free electricity can be imported into the system at any time. In a context where neighbouring countries transition to renewable-powered electricity systems, and given the correlation between renewable production signals on a regional scale [60,61], it seems unlikely that arbitrary amounts of electricity will be provided on demand in case of regional low-production events. In addition, historical wholesale prices used are particularly low, around 30€/MWh. In conclusion, increasing electricity import quotas would misrepresent system economics and overestimate system adequacy, which justifies this modelling choice.

5. Conclusion and future work

An optimisation-based framework has been proposed to tackle long-term centralised planning problems of multi-sector, integrated energy systems including electricity, hydrogen, natural gas, synthetic methane and carbon dioxide. The model selects and sizes the set of power generation, energy conversion and storage as well as carbon capture

technologies minimising the cost of supplying energy demand in the form of electricity, hydrogen, natural gas or synthetic methane across the power, heating, transportation and industry sectors whilst accounting for policy drivers, such as energy independence, carbon dioxide emissions reduction targets, or support schemes.

The model is illustrated by a case study evaluating the potential of sector coupling via power-to-gas and carbon capture technologies to achieve deep decarbonisation objectives in the Belgian context. Results, on the one hand, indicate that power-to-gas can only play a minor supporting role in cross-sector decarbonisation strategies in Belgium, as electrolysis plants are generally deployed in moderate quantities whilst methanation plants do not appear in any studied scenario. On the other hand, given the limited renewable potential, post-combustion and direct air carbon capture technologies appear to play an enabling role in any decarbonisation strategy. More precisely, in the absence of nuclear power plants, the economically-optimal system design relies on a mix of renewable-based technologies and fossil-based technologies equipped with post-combustion carbon capture for electricity generation, steam methane reformers equipped with carbon capture and electrolysis plants in small quantities for hydrogen production, natural gas imports to supply natural gas demand, and direct air carbon capture units to achieve ambitious carbon dioxide emissions reductions. It should be emphasised that although carbon capture technologies appear to play an enabling role, their deployment also exacerbates the dependence on fossil fuels. Finally, it has been observed that the saturation of the carbon dioxide export capacity has a substantial impact on electricity and hydrogen system design, pointing to the existence of nontrivial interactions between subsystems which must be carefully considered when planning and designing integrated energy systems.

In future work, from a modelling standpoint, adding a spatial dimension to the model and particularly including network models for different carriers would be an avenue worth investigating, as it would allow to quantify the extent to which congestion in carrier networks (and not only at their boundaries) and transmission system expansion costs impact system design. Moreover, in the current setup, demands for different carriers from the heating and transportation sectors, for example, have been defined exogenously. Endogenously assessing the applications for which each carrier is well-suited based on technological options, carrier properties and cost would offer a better insight into decarbonisation strategies. From a computational standpoint, the model, in its current state, remains tractable even on laptop computers. Exploring much larger model instances and solution methods such as decomposition methods on dedicated hardware would also be interesting. Alternatively, expanding the set of scenarios to consider technology cost reductions, tighter import/exports capacities or budgets, improved technical performance would allow for the evaluation of different sensitivities and ultimately yield valuable insights into long-term, multi-carrier, multi-sector system planning.

Conflict of interest

None declared.

Appendix A. Supplementary data

Supplementary data associated with this article can be found, in the online version, at https://doi.org/10.1016/j.epsr.2019.106039.

References

[1] M. O'Malley, B. Kroposki, B. Hannegan, H. Madsen, et al., Integrated Energy Systems: Defining and Describing the Value Proposition, Tech. Rep. National Renewable Energy Lab, Golden, CO, 2016.

[2] I.E. Agency, Status of Power System Transformation, (2018) (accessed 03.08.19), https://webstore.iea.org/download/summary/1041.

[3] A. Belderbos, Storage Via Power-To-Gas in Future Energy Systems: The Need for Synthetic Fuel Storage in Systems With High Shares of Intermittent Renewables (Ph.D. thesis, Katholieke Universiteit Leuven, Leuven, Belgium, 2019.

[4] G. Pleßmann, M. Erdmann, M. Hlusiak, C. Breyer, Global energy storage demand for a 100% renewable electricity supply, Energy Proc. 46 (2014) 22–31, https://doi.org/10.1016/j.egypro.2014.01.154 8th International Renewable Energy Storage Conference and Exhibition (IRES2013).

[5] D. Bogdanov, C. Breyer, North-east Asian super grid for 100 supply: optimal mix of energy technologies for electricity, gas and heat supply options, Energy Convers. Manag. 112 (2016) 176–190, https://doi.org/10.1016/j.enconman.2016.01.019.

[6] T. Brown, D. Schlachtberger, A. Kies, S. Schramm, M. Greiner, Synergies of sector coupling and transmission reinforcement in a cost-optimised, highly renewable European energy system, Energy 160 (2018) 720–739, https://doi.org/10.1016/j.energy.2018.06.222.

[7] K. Poncelet, E. Delarue, D. Six, J. Duerinck, W. D'haeseleer, Impact of the level of temporal and operational detail in energy-system planning models, Appl. Energy 162 (2016) 631–643, https://doi.org/10.1016/j.apenergy.2015.10.100.

[8] M. Berger, D. Radu, R. Fonteneau, G. Detienne, T. Deschuyteneer, D. Ernst, Centralised planning of national integrated energy system with power-to-gas and gas storages, 2018 Mediterranean Conference on Power Generation, Transmission, Distribution and Energy Conversion (MEDPOWER) (2018) 1–6.

[9] M. Berger, Optimal Multi-Carrier System Planning Repository. https://github.com/MathiasPBerger/MultiCarrierPlanning (accessed 03.08.19).

[10] P. Mancarella, MES (multi-energy systems): an overview of concepts and evaluation models, Energy 65 (2014) 1–17, https://doi.org/10.1016/j.energy.2013.10.041.

[11] B.H. Bakken, A.T. Holen, Energy service systems: integrated planning case studies, IEEE Power Engineering Society General Meeting, vol. 2 (2004) 2068–2073, https://doi.org/10.1109/PES.2004.1373245.

[12] M. Geidl, G. Andersson, A modeling and optimization approach for multiple energy carrier power flow, 2005 IEEE Russia Power Tech (2005) 1–7, https://doi.org/10.1109/PTC.2005.4524640.

[13] G. Chicco, P. Mancarella, From cogeneration to trigeneration: profitable alternatives in a competitive market, IEEE Trans. Energy Convers. 21 (1) (2006) 265–272, https://doi.org/10.1109/TEC.2005.858089.

[14] M. Qadrdan, J. Wu, N. Jenkins, J. Ekanayake, Operating strategies for a GB integrated gas and electricity network considering the uncertainty in wind power forecasts, IEEE Trans. Sustain. Energy 5 (1) (2014) 128–138, https://doi.org/10.1109/TSTE.2013.2274818.

[15] T.W.K. Mak, P.V. Hentenryck, A. Zlotnik, R. Bent, Dynamic compressor optimization in natural gas pipeline systems, INFORMS J. Comput. 31 (1) (2019) 40–65, https://doi.org/10.1287/ijoc.2018.0821.

[16] R. Bent, S. Blumsack, P. Van Hentenryck, C. Borraz-Sánchez, M. Shahriari, Joint electricity and natural gas transmission planning with endogenous market feedbacks, IEEE Trans. Power Syst. 33 (6) (2018) 6397–6409, https://doi.org/10.1109/TPWRS.2018.2849958.

[17] A. Zlotnik, L. Roald, S. Backhaus, M. Chertkov, G. Andersson, Coordinated scheduling for interdependent electric power and natural gas infrastructures, IEEE Trans. Power Syst. 32 (1) (2017) 600–610, https://doi.org/10.1109/TPWRS.2016.2545522.

[18] C. O'Malley, L. Roald, D. Kourounis, O. Schenk, G. Hug, Security assessment in gas-electric networks, 2018 20th Power Systems Computation Conference (PSCC 2018), IEEE, Dublin, Ireland, June 11-15, 2018, 2018, p. 8442923, https://doi.org/10.23919/PSCC.2018.8442923.

[19] J. Yang, N. Zhang, C. Kang, Q. Xia, Effect of natural gas flow dynamics in robust generation scheduling under wind uncertainty, IEEE Trans. Power Syst. 33 (2) (2018) 2087–2097, https://doi.org/10.1109/TPWRS.2017.2733222.

[20] M. Yan, Y. He, M. Shahidehpour, X. Ai, Z. Li, J. Wen, Coordinated regional-district operation of integrated energy systems for resilience enhancement in natural disasters, IEEE Trans. Smart Grid (2018) 1, https://doi.org/10.1109/TSG.2018.2870358.

[21] S. Clegg, P. Mancarella, Integrated modeling and assessment of the operational impact of power-to-gas (p2g) on electrical and gas transmission networks, IEEE Trans. Sustain. Energy 6 (4) (2015) 1234–1244, https://doi.org/10.1109/TSTE.2015.2424885.

[22] M. Qadrdan, M. Abeysekera, M. Chaudry, J. Wu, N. Jenkins, Role of power-to-gas in an integrated gas and electricity system in Great Britain, Int. J. Hydrogen Energy 40 (17) (2015) 5763–5775, https://doi.org/10.1016/j.ijhydene.2015.03.004.

[23] Y. Li, W. Liu, M. Shahidehpour, F. Wen, K. Wang, Y. Huang, Optimal operation strategy for integrated natural gas generating unit and power-to-gas conversion facilities, IEEE Trans. Sustain. Energy 9 (4) (2018) 1870–1879, https://doi.org/10.1109/TSTE.2018.2818133.

[24] M.H. Shams, M. Shahabi, M.E. Khodayar, Risk-averse optimal operation of multiple-energy carrier systems considering network constraints, Electr. Power Syst. Res. 164 (2018) 1–10, https://doi.org/10.1016/j.epsr.2018.07.022.

[25] C. Tovar-Ramírez, C. Fuerte-Esquivel, A.M. Mares, J. Sánchez-Gardu no, A generalized short-term unit commitment approach for analyzing electric power and natural gas integrated systems, Electr. Power Syst. Res. 172 (2019) 63–76, https://doi.org/10.1016/j.epsr.2019.03.005.

[26] M. Qadrdan, R. Fazeli, N. Jenkins, G. Strbac, R. Sansom, Gas and electricity supply implications of decarbonising heat sector in GB, Energy 169 (2019) 50–60, https://doi.org/10.1016/j.energy.2018.11.066.

[27] M. Geidl, G. Andersson, Optimal coupling of energy infrastructures, 2007 IEEE Lausanne Power Tech (2007) 1398–1403, https://doi.org/10.1109/PCT.2007.4538520.

[28] A. Belderbos, E. Delarue, W. D'haeseleer, Possible role of power-to-gas in future energy systems, 2015 12th International Conference on the European Energy Market (EEM) (2015) 1–5, https://doi.org/10.1109/EEM.2015.7216744.

[29] P. Gabrielli, M. Gazzani, E. Martelli, M. Mazzotti, Optimal design of multi-energy

systems with seasonal storage, Appl. Energy 219 (2018) 408–424, https://doi.org/10.1016/j.apenergy.2017.07.142.
[30] M. Panto, Stochastic generation-expansion planning and diversification of energy transmission paths, Electr. Power Syst. Res. 98 (2013) 1–10, https://doi.org/10.1016/j.epsr.2012.12.017.
[31] M. Chaudry, N. Jenkins, M. Qadrdan, J. Wu, Combined gas and electricity network expansion planning, Appl. Energy 113 (2014) 1171–1187, https://doi.org/10.1016/j.apenergy.2013.08.071.
[32] B. Odetayo, J. MacCormack, W. Rosehart, H. Zareipour, A chance constrained programming approach to integrated planning of distributed power generation and natural gas network, Electr. Power Syst. Res. 151 (2017) 197–207, https://doi.org/10.1016/j.epsr.2017.05.036.
[33] B. Zhao, A.J. Conejo, R. Sioshansi, Coordinated expansion planning of natural gas and electric power systems, IEEE Trans. Power Syst. 33 (3) (2018) 3064–3075, https://doi.org/10.1109/TPWRS.2017.2759198.
[34] B. Zhao, Electricity-Gas Systems: Operations and Expansion Planning Under Uncertainty (Ph.D. thesis), The Ohio State University, Columbus, Ohio, USA, 2018.
[35] C. He, L. Wu, T. Liu, Z. Bie, Robust co-optimization planning of interdependent electricity and natural gas systems with a joint n-1 and probabilistic reliability criterion, IEEE Trans. Power Syst. 33 (2) (2018) 2140–2154, https://doi.org/10.1109/TPWRS.2017.2727859.
[36] D.S.T. Brown, J. Hörsch, Pypsa: Python for power system analysis, J. Open Res. Softw. 6 (1) (2018) 4.
[37] D. Dominkovic, I. Bacekovic, B. Cosic, G. Krajacic, T. Pukec, N. Duic, N. Markovska, Zero carbon energy system of South East Europe in 2050, Appl. Energy 184 (2016) 1517–1528, https://doi.org/10.1016/j.apenergy.2016.03.046.
[38] M. Götz, J. Lefebvre, F. Mörs, A.M. Koch, F. Graf, S. Bajohr, R. Reimert, T. Kolb, Renewable power-to-gas: a technological and economic review, Renew. Energy 85 (2016) 1371–1390, https://doi.org/10.1016/j.renene.2015.07.066.
[39] Air Liquide S.A., Technology Handbook. https://www.engineering-airliquide.com/sites/activity_eandc/files/2018/03/28/air-liquide-technology-handbook-march-2018.pdf (accessed 03.08.19).
[40] D. Bonaquist, Analysis of Carbon Dioxide Emissions, Reductions, and Capture for Large-Scale Hydrogen Production Plants, (2018) (accessed 03.08.19), https://www.praxair.com/-/media/corporate/praxairus/documents/reports-papers-case-studies-and-presentations/our-company/sustainability/praxair-co2-emissions-reduction-capture-white-paper.pdf?la=en&rev=dc79ff3c7b4c4974a1328c7660164765.
[41] J. Jechura, Hydrogen from Natural Gas via Steam Methane Reforming, (2015) (accessed 03.08.19), https://inside.mines.edu/jjechura/EnergyTech/07_Hydrogen_from_SMR.pdf.
[42] D.W. Keith, G. Holmes, D.S. Angelo, K. Heidel, A process for capturing CO_2 from the atmosphere, Joule 2 (8) (2018) 1573–1594, https://doi.org/10.1016/j.joule.2018.05.006.
[43] E.S. Rubin, J.E. Davison, H.J. Herzog, The cost of co2 capture and storage, Int. J. Greenhouse Gas Control 40 (2015) 378–400, https://doi.org/10.1016/j.ijggc.2015.05.018 Special Issue commemorating the 10th year anniversary of the publication of the Intergovernmental Panel on Climate Change Special Report on CO2 Capture and Storage.
[44] N. DiOrio, A. Dobos, S. Janzou, Economic Analysis Case Studies of Battery Energy Storage with SAM. https://www.nrel.gov/docs/fy16osti/64987.pdf.
[45] T. Market, K. Bennion, W. Krammer, J. Bryan, J. Giedd, Field Testing Plug-In Hybrid Electric Vehicles With Charge Control Technology in the Xcel Energy Territory, Tech. Rep, National Renewable Energy Laboratory, Golden, CO, 2009.
[46] M.D. Galus, R.A. Waraich, F. Noembrini, K. Steurs, G. Georges, K. Boulouchos, K.W. Axhausen, G. Andersson, Integrating power systems, transport systems and vehicle technology for electric mobility impact assessment and efficient control, IEEE Trans. Smart Grid 3 (2) (2012) 934–949, https://doi.org/10.1109/TSG.2012.2190628.
[47] I. Pavic, T. Capuder, N. Holjevac, I. Kuzle, Role and impact of coordinated EV charging on flexibility in low carbon power systems, 2014 IEEE International Electric Vehicle Conference (IEVC) (2014) 1–8, https://doi.org/10.1109/IEVC.2014.7056172.
[48] Elia, Electricity Scenarios for Belgium Towards 2050 – Elia's Quantified Study on the Energy Transition in 2030 and 2040, (2017) (accessed 03.08.19), https://www.elia.be//media/files/Elia/About-Elia/Studies/20171114_ELIA_4584_AdequacyScenario.pdf.
[49] Elia, Power Generation, (2019) (accessed 03.08.19), http://www.elia.be/en/grid-data/power-generation.
[50] Elia, Load and Load Forecasts – Total Load, (2019) (accessed 03.08.19), http://www.elia.be/en/grid-data/Load-and-Load-Forecasts/total-load.
[51] Fluxys, Flow Data – Ex-Post Domestic Exit Point Information, (2019) (accessed 03.08.19), https://gasdata.fluxys.com/transmission-ztp-trading-services/flow-data/.
[52] Statbel, Energy Consumption Statistics – Global Energy Balance, (2019) (accessed 03.08.19), https://bestat.statbel.fgov.be/bestat/.
[53] P.N.N. Laboratory, Merchant Hydrogen Production in Europe, (2014) (accessed 03.08.19), https://h2tools.org/hyarc/hydrogen-data/merchant-hydrogen-production-europe.
[54] E. Gysels, The Role of Green Hydrogen in Belgium's Future Energy System (Master's thesis), Aalborg University, 2018.
[55] P.I.C. Flanders, Power-to-Gas, Roadmap for Flanders, (2015) (accessed 03.08.19), http://www.power-to-gas.be/roadmap-study.
[56] E.E. Agency, EEA Greenhouse Gas – Data Viewer, (2019) (accessed 03.08.19), https://www.eea.europa.eu/data-and-maps/data/data-viewers/greenhouse-gases-viewer.
[57] I.P. on Climate Change (IPCC), IPCC Emissions Factor Database, (2006) (accessed 03.08.19), https://ghgprotocol.org/Third-Party-Databases/IPCC-Emissions-Factor-Database.
[58] R. Span, W. Wagner, A new equation of state for carbon dioxide covering the fluid region from the triple-point temperature to 1100 K at pressures up to 800 MPa, J. Phys. Chem. Ref. Data 25 (6) (1996) 1509–1596, https://doi.org/10.1063/1.555991.
[59] T. Schröder, W. Kuckshinrichs, Value of lost load: An efficient economic indicator for power supply security? A literature review, Front. Energy Res. 3 (2015) 55, https://doi.org/10.3389/fenrg.2015.00055.
[60] D. Radu, M. Berger, R. Fonteneau, S. Hardy, X. Fettweis, M.L. Du, P. Panciatici, L. Balea, D. Ernst, Complementarity assessment of south Greenland katabatic flows and west Europe wind regimes, Energy 175 (2019) 393–401, https://doi.org/10.1016/j.energy.2019.03.048.
[61] M. Berger, D. Radu, R. Fonteneau, R. Henry, M. Glavic, X. Fettweis, M.L. Du, P. Panciatici, L. Balea, D. Ernst, Critical Time Windows for Renewable Resource Complementarity Assessment, (2018) arXiv:1812.02809.